Final Draft

of the original manuscript

Wang, J.; Rahman, M.; Abetz, C.; Abetz, V.:

Bovine serum albumin selective integral asymmetric isoporous membrane.

In: Journal of Membrane Science. Vol. 604 (2020) 118074.

First published online by Elsevier: 23.03.2020

https://dx.doi.org/10.1016/j.memsci.2020.118074

Bovine serum albumin selective integral asymmetric isoporous membrane

Jiali Wang[1], Md. Mushfequr Rahman[1], Clarissa Abetz[1], Volker Abetz[1,2]*

[1]Helmholtz-Zentrum Geesthacht, Institute of Polymer Research, Max-Planck-Str. 1, 21502 Geesthacht, Germany

[2]Universität Hamburg, Institute of Physical Chemistry, Martin-Luther-King-Platz 6, 20146 Hamburg, Germany

*Corresponding author. Email address: volker.abetz@hzg.de

Abstract

Separation of bovine serum albumin (BSA) and hemoglobin (Hb), two proteins with almost identical molecular weight, has been a big challenge for more than two decades. Using traditional ultrafiltration membranes separation of these proteins is possible only at the isoelectric point of one protein via electrostatic repulsion between the membrane and the other protein. Here we introduce an integral asymmetric isoporous membrane from polystyrene-*block*-poly(2-hydroxyethyl methacrylate-*ran*-2-(succinyloxy)ethyl methacrylate) (PS-*b*-P(HEMA-*r*-SEMA)) having random –OH and –COOH groups along the pore walls prepared by a method which combines solvent induced self-assembly of the block copolymer and nonsolvent induced phase separation (SNIPS). The membrane consists of soft isoporous channels due to swelling of the P(HEMA-*r*-SEMA) blocks in a hydrated state. The effective pore size of the membrane in a hydrated state is significantly lower compared to that in a dry state. These soft channels allow the permeation of BSA while retaining Hb at constant pH 7.4 where both proteins are negatively charged. In comparison to 22 commercial and in-house prepared membranes the PS-*b*-P(HEMA-*r*-SEMA) membrane presents unprecedented ideal selectivity of BSA over Hb ($\psi_{BSA/Hb} = 16$). Unlike the conventional technique in this case the electroneutrality of one protein is not mandatory which will provide significantly easier handling.

1. Introduction

Membrane technology has earned a reputation as an effective technique for fractionation of proteins over other conventional techniques e.g. chromatography in food and biotechnology industries, owing to the mild conditions of operation, readily scalable processes and good separation properties. The traditional ultrafiltration (UF) and microfiltration (MF) membranes are already commercially feasible for the separation of proteins mainly dependent on the large molecular size differences, for instance fractionation of casein and whey proteins in the dairy food industry. However, fractionation of proteins having identical or very similar molecular weights is still confronted with a low selectivity of the current commercially available membranes due to irregular pores and broad pore size distributions. Bovine serum albumin (BSA) and hemoglobin (Hb) are the most widely studied protein pair having almost identical molecular weights. [1-7] More than two decades ago Eijndhoven *et al*. [1] demonstrated that a separation factor of more than 70 can be achieved for this protein pair by taking advantage of their significantly different isoelectric points using a commercial polyethersulfone membrane. The separation was performed at the isoelectric point of Hb and at a very low ionic strength which resulted in an easy permeation of the neutral Hb and a strong electrostatic exclusion of BSA. Till now this technique has been extensively utilized for the separation of BSA and Hb. Several innovative techniques to prepare membranes having narrow pore size distribution and diverse chemical functionality have been reported in the last two decades. But in most cases BSA has been separated from Hb or other proteins (e.g. immunoglobulin) at the isoelectric point of one of the proteins. [5, 8] Since this technique relies on the electroneutrality of one of the proteins, a slight deviation of the pH from the isoelectric point results in a dramatic reduction of the selectivity which is not ideal for large scale applications. [2] In this work we report a new integral asymmetric isoporous membrane which shows excellent selectivity of BSA over Hb and catalase (Cat) at pH 7.4 where all three proteins have a net negative charge. The membrane was prepared by a method which combines self-assembly of block copolymer and nonsolvent induced phase separation (SNIPS). [9-16] Unlike the traditional homopolymer membranes prepared by nonsolvent induced phase separation (NIPS), the SNIPS membranes have highly uniform pore sizes and narrow pore size distributions. These features have promoted the SNIPS membranes as the next-generation membranes for separation of biomolecules and water purification in the last decade. [17-23] Specially the protein separation performance of the SNIPS membranes has attracted significant attention [5, 6, 8, 24, 25]. The potential applications of SNIPS membranes have led the researchers to explore and improve the properties of SNIPS membranes in many aspects e.g. mechanical stability, [26] thermal stability, [27, 28] surface functionality, [29, 30] stimuli responsiveness [5, 8, 24-26, 31, 32] etc. Several strategies to systematically tune the pore size of the SNIPS membranes have been reported, e.g. changing molecular weights and compositions of the block copolymers, [33] blending two block copolymers of different molecular weights and compositions, [34] selective postmodification of the pore-forming block of the prepared membranes, [35] thermal annealing of the prepared membranes, [35] conformal coating/deposition of inorganic layer on the SNIPS membranes, [15, 36] etc. But most of the SNIPS membrane studies have been focused on diblock or triblock copolymers where the pore forming block was composed of vinylpyridine repeating units. Recently, successful fabrication of SNIPS membranes having hydroxyl functional groups along the pore walls were reported. [35, 37, 38] Herein, we report for the first time a one-step fabrication of an isoporous membrane having random distribution of hydroxyl and carboxylic groups along the pore walls using polystyrene-*block*-poly(2-hydroxyethyl methacrylate-*ran*-2-(succinyloxy)ethyl methacrylate) (PS-*b*-P(HEMA-*r*-SEMA)) block copolymers. No membrane postmodification step was required as the block copolymer itself was tailored with the desired

functionality. The new integral asymmetric isoporous membrane demonstrates its strong potential in separating biomolecules of similar size on the example of BSA and Hb.

2. Experimental

2.1. Synthesis of diblock copolymers

PS-*b*-PHEMA block copolymer was prepared by sequential anionic polymerization following a protocol reported before (**Supporting Information, Scheme S1**). [35, 39] Five batches of PS-*b*-PHEMA diblock copolymers were reacted with 5-fold excess (molar ratio) of succinic anhydride in anhydrous pyridine for a series of reaction time at room temperature under argon without any catalyst (**Supporting information, Scheme S3, S4**). [40] The obtained polymers were precipitated in methanol three times and dried under vacuum at 50 °C until constant weight.

2.2. Membranes fabrication via SNIPS

The casting solutions of the obtained polymers were prepared in a mixture of THF/DMF/DOX with or without the addition of salts. After stirring for 48 h the casting solution was manually cast using a doctor blade with a gap height of 200 μm on a glass plate or a polyester nonwoven support. The concentration of casting solution, the composition of the solvent mixture, the evaporation time before immersing into a water bath and the addition of salts were optimized in order to obtain the isoporous structure for each batch of polymers. After casting the prepared membranes were immersed in a water bath for 20 min to ensure the complete exchange between the solvent mixture and water. Since the PHEMA and PSEMA segments are very sensitive to humidity, the relative humidity of air (RH) was precisely controlled below 20% during the whole process of casting by using a glove box equipped with N_2 flow. The membranes were dried under vacuum at 50 °C for 4 days to remove all residual solvents.

2.3. Characterization of polymers and membranes

To facilitate the characterization of PS-*b*-PHEMA diblock copolymer, the hydroxyl groups of the PHEMA segment were protected by benzoic anhydride (**Supporting Information, Scheme S2**). Dispersity index (Đ) and molecular weights of the PS-precursor and the benzoylated PS-*b*-PHEMA (PS-*b*-P(HEMA-Bz)) diblock copolymers were determined by size exclusion chromatography (SEC). The characteristic peaks of the different blocks were quantitatively determined by proton nuclear magnetic resonance (^{1}H-NMR) (300 MHz, Bruker, Rheinstetten, Germany) using $CDCl_3$ and DMSO-d6 as solvents with the internal standard tetramethylsilane (TMS). The membrane morphology was investigated by scanning electron microscopy (SEM) (LEO Gemini 1550 VP from Carl ZEISS, Oberkochen, Germany) at an acceleration voltage of 3 kV. The average pore diameter (D_p) was measured by ImageJ 1.46 (Wayne Rasband, National Institute of Health, Madison, WI, USA) on the basis of the SEM results. The dynamic viscosities of polymer solutions were measured with the rotational viscometer EuroPhysics Rhoe2000 using a C25-1 cone/plate geometry. The measurements were performed at a constant shear rate of 200 s^{-1} at 20 °C.

2.4 Membrane performance measurements

The pure water permeance measurements were conducted in a dead-end mode at a constant feed pressure of 2 bar and 3 bar at 20 °C as shown in **Supporting Information, Section 7**. All the membranes were soaked in demineralized water for 24 h before measurement to ensure the sufficient swelling of membrane. All experiments were performed at least in triplicate by using three individual single modules.

The water permeance measurements as a function of pH were performed in the pH range of 3 ~ 13 in a dead-end mode with continuously stirring at a trans-membrane pressure of 1 bar at 20 °C as shown in **Supporting Information, Section 7**. Permeance at each pH value was measured three times for 20 minutes and the average value was calculated. All the membranes were soaked in demineralized water for 24 h before measurement to ensure the sufficient swelling of membrane. Each measurement was conducted in triplicate using three individual single modules.

The water permeance (J) is calculated as follows,

$$J = \frac{\Delta V}{A \cdot \Delta t \cdot \Delta p}$$

Where, ΔV is the volume change of water permeance between two mass measurements, A is the effective membrane area, Δt is the time interval between two mass measurements, Δp is the trans-membrane pressure.

The protein retention measurements were performed in a dead-end mode with continuously stirring under a trans-membrane pressure of 2 bar at 20 °C (**Supporting Information, Section 7**). The retention property of membranes was investigated using BSA, Hb and Cat. The feed solution of proteins was all freshly prepared in phosphate-buffered saline (PBS, pH = 7.4) for retention measurement. PBS solution was first supplied to the membranes for 1 h at the trans-membrane pressure of 2 bar in order to exclude the influence of buffer, and then the 1 g L^{-1} feed solution of proteins was provided at the same pressure for 2 h. Each measurement was conducted three times. The concentration of proteins in the feed (C_f) and permeate (C_p) was determined by UV-vis spectrophotometer (GENESYS 10S, Thermo Scientific) and the retention ratio was calculated following the equation showed below:

$$R\% = \left(1 - \frac{C_p}{C_f}\right) \times 100\%$$

Where, C_p and C_f are concentrations of proteins in permeate and feed, respectively.

Solute transmission is usually expressed in terms of the observed percentage transmission (τ_{Obs}). [41]

$$\tau_{Obs} = \frac{C_p}{C_f} \times 100$$

The ideal selectivity (ψ) of one protein from another one is expressed as: [41]

$$\psi = \frac{(\tau_{Obs})_i}{(\tau_{Obs})_j}$$

where $(\tau_{Obs})_i$and $(\tau_{Obs})_j$are the observed percentage transmissions of two different proteins.

3. Results and discussion

3.1. Block copolymer synthesis and optimization of membrane casting condition

Polystyrene-*block*-poly(2-hydroxyethyl methacrylate), PS_{94}-*b*-$PHEMA_6^{149}$ was synthesized via sequential anionic polymerization of styrene and 2-(trimethylsilyloxy)ethyl methacrylate followed by hydrolytic cleavage of the trimethylsilyloxy group using concentrated hydrochloric acid (**Fig. 1**). For the acronym of polymers subscripts indicate weight fraction (%) of the blocks; superscripts indicate the molecular weight (kg mol^{-1}). The hydroxyl moieties of the PHEMA block was esterified with succinic anhydride [40] (**Fig. 1**) to obtain four polystyrene-*block*-poly(2-hydroxyethyl methacrylate-*ran*-2-succinyloxyethyl methacrylate) (PS-*b*-P(HEMA-*r*-SEMA)) having 5 ~ 57 wt % randomly distributed SEMA moieties. A polystyrene-*block*-poly(2-succinyloxyethyl methacrylate) (PS-*b*-PSEMA) was also synthesized by complete esterification of the PHEMA block. The compositions and molecular weights of the 6 synthesized block copolymers are listed in the **Supporting Information (Table S2)**.

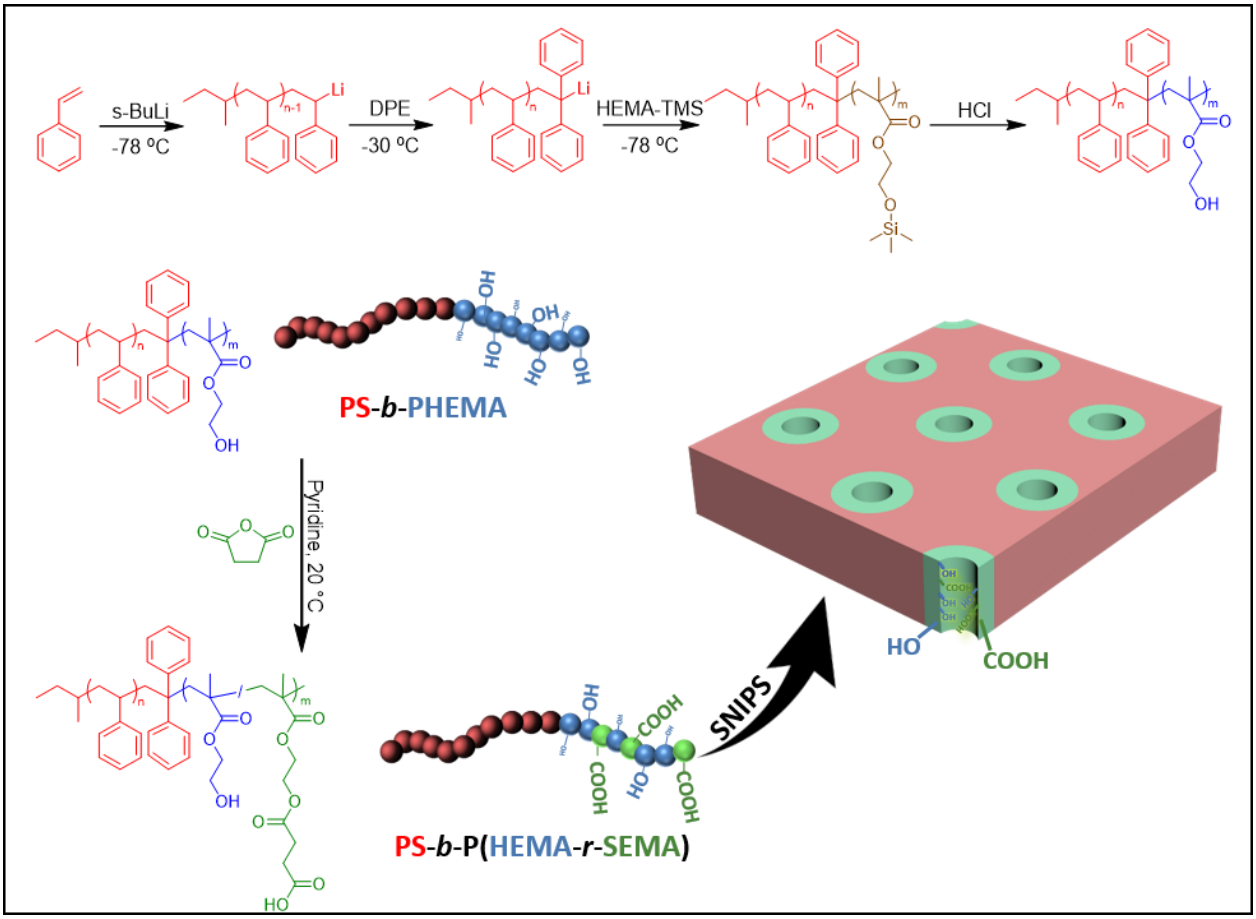

Fig. 1. Synthesis route of polystyrene-*block*-poly(2-hydroxyethyl methacrylate) (PS-*b*-PHEMA) and polystyrene-*block*-poly(2-hydroxyethyl methacrylate-*ran*-2-succinyloxyethyl methacrylate) (PS-*b*-P(HEMA-*r*-SEMA)). Schematic representation of the isoporous top layer of PS-*b*-P(HEMA-*r*-SEMA) membrane prepared by SNIPS.

All 6 polymers were used to fabricate membranes via SNIPS. In this method a rather viscous polymer solution is cast on a glass or porous support using a doctor blade followed by a short evaporation time and subsequent precipitation in a water bath (**Fig. 2a**). An asymmetric membrane having hexagonally close-packed vertically aligned isoporous channels on top of a

highly porous spongy sublayer can be obtained upon optimization of the casting parameters e.g. concentration of the casting solution, composition of the solvent system, evaporation time prior to the precipitation bath etc. In a previous study [35] we obtained isoporous SNIPS membranes from a PS_{91}-*b*-$PHEMA_9^{97}$ using a ternary solvent mixture of THF/DMF/DOX (2:1:1, weight ratio). However, an integral asymmetric isoporous morphology was not obtained from the synthesized PS_{94}-*b*-$PHEMA_6^{149}$ using a THF/DMF/DOX (2:1:1) solvent mixture (**Supporting information, Fig. S3**). In a PS-*b*-PHEMA SNIPS membrane the short PHEMA block forms the open pores of the isoporous top layer while the PS block forms the matrix. The molecular weight and the composition of the block copolymer largely determines the morphology of the isoporous layer of a SNIPS membrane. The PHEMA block content of the synthesized PS_{94}-*b*-$PHEMA_6^{149}$ was probably too low to form an isoporous top layer via SNIPS. The content of the pore forming block gradually increased with the degree of esterification and the incompatibility between the blocks changed. These properties of the polymers have a crucial impact on the SNIPS membrane morphology and thereby to determine the optimum casting parameters. Using a THF/DMF/DOX (2:1:1) solvent mixture the desired hexagonally packed isoporous surface was not obtained from any of the synthesized polymers (**Supporting information, Fig. S4**). A membrane with relatively narrow surface pore size distribution and high surface porosity was obtained from a 22 wt % PS_{92}-*b*-$P(HEMA_{63}$-*r*-$SEMA_{37})_8^{150}$ casting solution in THF/DMF/DOX (2:1:1) at the evaporation time of 25 s (**Fig. 2b**). Therefore, the PS_{92}-*b*-$P(HEMA_{63}$-*r*-$SEMA_{37})_8^{150}$ was used to further optimize the casting parameters on a glass plate. The formation of the isoporous top layer of an ideal SNIPS membrane is largely dictated by the solvent evaporation. After casting the polymer solution one of the solvents of the ternary mixture has to evaporate fast in order to drive the self-assembly of the block copolymer domains perpendicular to the surface. At the same time another high boiling solvent should selectively keep the pore forming block in a swollen state. Upon precipitation in the water bath the pore forming blocks collapse to form the pores. This process is schematically represented in **Fig. 2a**. According to the solubility parameters among the solvents the polar DMF is more selective for the $P(HEMA_{63}$-*r*-$SEMA_{37})$ blocks while THF and DOX are more selective for PS (**Supporting Information, Table S4 and S5**). The evaporation rate of THF is significantly higher than DOX and DMF. Hence, while casting PS_{92}-*b*-$P(HEMA_{63}$-*r*-$SEMA_{37})_8^{150}$ membranes the evaporation of more volatile THF mostly drives the assembly of the domains perpendicular to the surface of the membrane and DMF is responsible to keep the $P(HEMA_{63}$-*r*-$SEMA_{37})$ block in a swollen state before precipitation. For the THF/DMF/DOX (2:1:1) ternary solvent mixture the best surface morphology was obtained from a 22 wt % solution at the evaporation time of 25 second (**Fig. 2b**). From the symmetry of the pores it is clear that the self-assembly of the block copolymer domains perpendicular to the surface of membrane took place during the solvent evaporation time. But some of the $P(HEMA_{63}$-*r*-$SEMA_{37})$ domains did not produce open pores. The surface pore size distribution of this membrane was also significantly higher than the surface pore size distribution of an ideal SNIPS membrane. Therefore, a higher DMF containing ternary solvent mixture THF/DMF/DOX (1:1:1) was used for further casting. The concentration of the polymeric solution and the evaporation time prior to the precipitation bath was optimized (**Supporting Information, Fig. S5**). The highest surface porosity was obtained for a membrane casted from a 21 wt % solution in THF/DMF/DOX (1:1:1) at the evaporation time of 20 s (**Fig. 2c**). This change of morphology is a result of several simultaneous phenomena. But it is evident that a higher amount of DMF in the solvent mixture kept the $P(HEMA_{63}$-*r*-$SEMA_{37})$ blocks in a sufficiently swollen state just before precipitation in the water bath.

Addition of complexing metal ions, [42, 43] or hydrogen bonding organic molecules [44, 45] can improve the structure formation of the SNIPS membranes. The isoporous structure of the

PS_{92}-*b*-P($HEMA_{63}$-*r*-$SEMA_{37}$)$_8^{150}$ membrane was further improved by tuning the viscosity using $CuCl_2$, $CuAc_2$ and $MgAc_2$. For example the viscosity of the 21 wt % PS_{92}-*b*-P($HEMA_{63}$-*r*-$SEMA_{37}$)$_8^{150}$ solution in THF/DMF/DOX (1:1:1) increased from 197 Pa s to 398 Pa s due to addition of 0.1 wt % $CuCl_2$ which resulted in a relatively open porous structure at the surface of the membrane (**Fig. 2d**). An increase of viscosity of the casting solution is accompanied with a restricted polymer chain mobility. The addition of salts may facilitate the formation of open porous structure only within a viscosity zone where the mobility of the block copolymer segment is enough for the alignment of the domains perpendicular to the membrane surface. The surface porosity drops significantly if the viscosity becomes too high due to addition of salts in the casting solution. (**Supporting Information, Fig. S6**) In this study a 20 wt % solution of PS_{92}-*b*-P($HEMA_{63}$-*r*-$SEMA_{37}$)$_8^{150}$ in THF:DMF:DOX (1:1:1) containing 0.1 wt % $MgAc_2$ was the optimum casting solution which had a viscosity of 456 Pa s (**Fig. 2e**). $MgAc_2$ is more environmentally friendly compared to the toxic copper salts. We obtained the desired morphology of a free-standing membrane cast on a glass plate using this solution for an optimum evaporation time of 25 seconds.

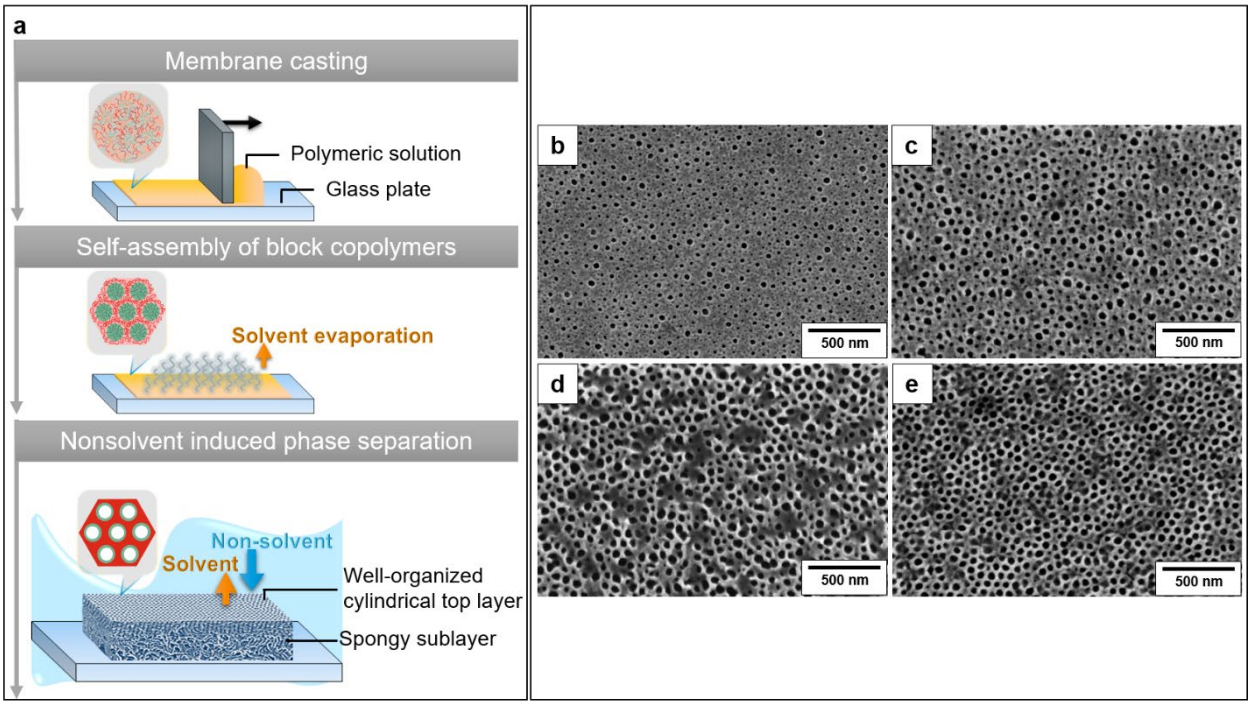

Fig. 2. a) Scheme of SNIPS method on the glass plate; b) 22 wt % PS_{92}-*b*-P($HEMA_{63}$-*r*-$SEMA_{37}$)$_8^{150}$ casting solution in THF/DMF/DOX (2:1:1) at the evaporation time of 25 s; c) 21 wt % casting solution in THF/DMF/DOX (1:1:1) at the evaporation time of 20 s; d) 21 wt % casting solution with 0.1 wt % $CuCl_2$ at the evaporation time of 20 s; e) 20 wt % casting solution with 0.1 wt % $MgAc_2$ at the evaporation time of 25 s.

A PS_{92}-*b*-P($HEMA_{63}$-*r*-$SEMA_{37}$)$_8^{150}$ integral asymmetric isoporous membrane was prepared on a nonwoven porous support (**Fig. 3e**) using the optimized casting parameters on the glass plate. SEM images of the top surface shows that PS_{92}-*b*-P($HEMA_{63}$-*r*-$SEMA_{37}$)$_8^{150}$ membrane features hexagonally packed vertically aligned isoporous channels on top of spongy sublayer (**Fig. 3c**). A highly open porous substructure was observed throughout the cross-section of the membrane (**Supporting Information**, **Fig. S7**).

3.2. Water permeance of the PS-*b*-P(HEMA-*r*-SEMA) membrane

In dry state the average pore size at the surface of the membrane was 37 ± 7 nm. But it must be noted that in a hydrated state the pore forming P($HEMA_{63}$-*r*-$SEMA_{37}$) block of the membrane swells and the isoporous channels become significantly smaller compared to what is observed by SEM investigation in a completely dry state (**Fig. 3c**). The effective pore size depends on the extent of swelling of the pore forming P($HEMA_{63}$-*r*-$SEMA_{37}$) blocks. Before presenting the results on protein separation of the PS_{92}-*b*-P($HEMA_{63}$-*r*-$SEMA_{37}$)$_8^{150}$ integral asymmetric isoporous membrane first the water permeance as a function of pH was studied. **Fig. 3b** shows the water permeance for increasing and decreasing pH. It can be clearly seen that above pH=10 the permeance drops strongly and then increases again. This can be explained by a strong swelling of the pore forming blocks due to hydrolysis of some intramolecular ester linkages formed between HEMA and SEMA or anhydride functions formed by two SEMA groups prior to membrane casting. After hydrolysis of the anhydride linkages at slightly larger pH also the ester linkages between HEMA and succinic moieties are hydrolysed. To check this interpretation a PS_{92}-*b*-P($HEMA_{63}$-*r*-$SEMA_{37}$)$_8^{150}$ powder was immersed in an aqueous solution (pH=13) for 20 min and a PS-*b*-PHEMA diblock copolymer (**Supporting Information, Fig. S15**) was obtained due to complete hydrolysis of the ester linkages (^{1}H-NMR spectra shown in **Fig. 3a**). This reaction also occurred on the PS_{92}-*b*-P($HEMA_{63}$-*r*-$SEMA_{37}$)$_8^{150}$ membrane during determination of water flux at an alkaline pH. The irreversible removal of the succinic moiety also leads to an increased water permeance level upon lowering the pH, which is higher for the PS-*b*-PHEMA as compared to the PS_{92}-*b*-P($HEMA_{63}$-*r*-$SEMA_{37}$)$_8^{150}$. This can be explained in the following way: The trend of water permeance suggests that in the pH range 3 to 10 the pore forming P($HEMA_{63}$-*r*-$SEMA_{37}$) blocks were in a rather collapsed state while at pH 11 and 12 the pore forming blocks adopted a rather stretched conformation which caused the decrease of water permeance. However, as the pK_a value of SEMA monomer is ~4.5 [46] the swelling of the P($HEMA_{63}$-*r*-$SEMA_{37}$) blocks at pH 11 and 12 cannot occur merely due to the pH responsiveness of the carboxylic moieties. The sudden swelling of the P($HEMA_{63}$-*r*-$SEMA_{37}$) blocks is possibly induced by the hydrolysis of the before mentioned intramolecular anhydride or ester linkages, complexation of the $MgAc_2$ additives with the functional groups of P($HEMA_{63}$-*r*-$SEMA_{37}$) blocks etc. [46] At pH 13 the water permeance increased dramatically above 400 L h^{-1} m^{-2} bar^{-1}as the SEMA repeating units were hydrolysed back to HEMA due to cleavage of the ester linkage (**Fig. 3a**). Therefore, there was no significant change of water permeance while the pH was gradually reduced from 13 to 3 (**Fig. 3b**). The integral asymmetric morphology of the membrane was not destroyed but the porosity and the dry state pore diameter (44 ± 12 nm) of the membrane increased due to hydrolysis (**Fig. 3d**). As the effective pore size of the membrane were higher after hydrolysis water permeance was also higher (**Fig. 3b)**. It is worth mentioning that it was not possible to obtain an integral asymmetric isoporous PS_{94}-*b*-$PHEMA_6^{149}$ membrane by SNIPS (**Supporting Information, Fig. S3**). These results demonstrate the potential of using a sacrificial succinate moiety to achieve a highly porous integral asymmetric PS-*b*-PHEMA membrane to overcome the limitation to directly cast a PS-*b*-PHEMA membrane by SNIPS due to low PHEMA content.

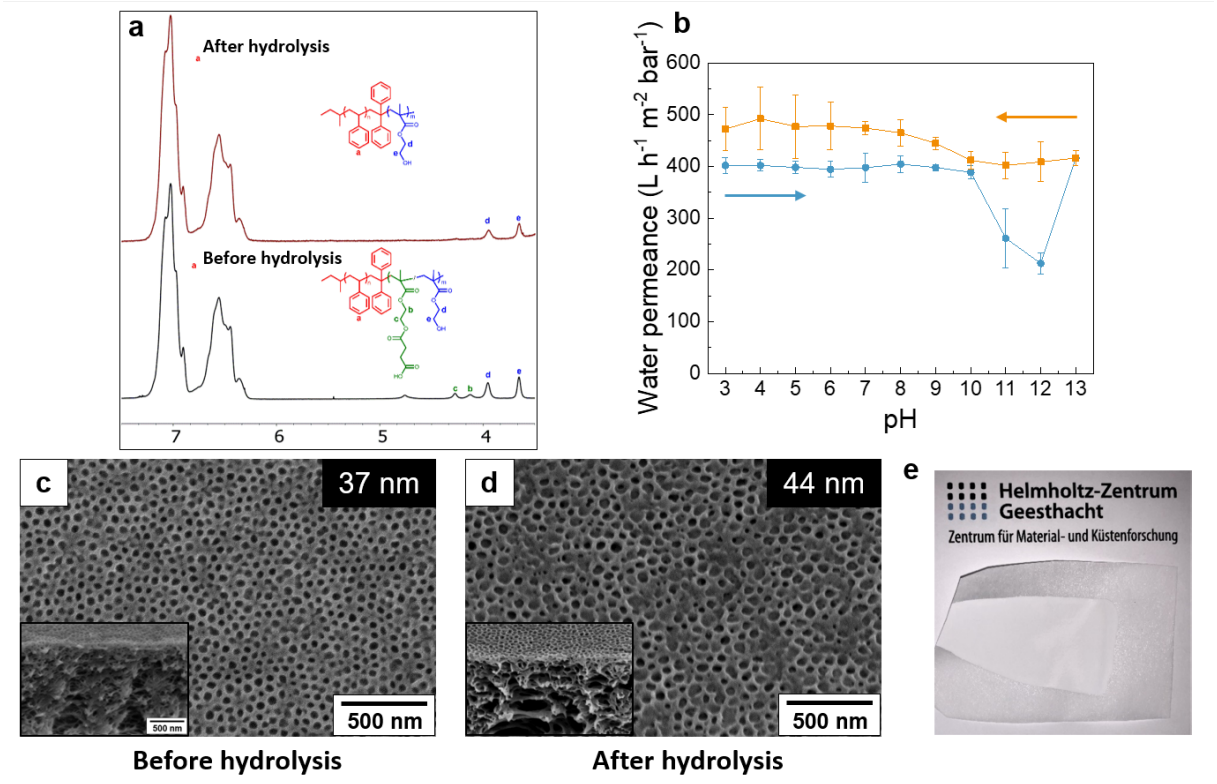

Fig. 3. a) ^{1}H-NMR spectra of PS_{92}-*b*-P($HEMA_{63}$-*r*-$SEMA_{37}$)$_8^{150}$ before and after pH treatment at pH=13 for 20 min in $CDCl_3$ and DMSO-d6 (volume ratio of 1/1) with internal standard TMS; b) Water permeance of membranes as a function of pH at a trans-membrane pressure of 1 bar at 20 °C; c) SEM images of the top surface and the cross-section membrane prepared from 20 wt % PS_{92}-*b*-P($HEMA_{63}$-*r*-$SEMA_{37}$)$_8^{150}$ casting solution in THF/DMF/DOX (1:1:1) with 0.1 wt % $MgAc_2$ at the evaporation time of 25 s which was casted on the nonwoven support; d) SEM images of the top surface and the cross-section membrane after water permeance measurement as a function of pH; e) The photo of PS_{92}-*b*-P($HEMA_{63}$-*r*-$SEMA_{37}$)$_8^{150}$ membrane cast on a nonwoven support.

3.3. Protein separation

The single protein retention of three bovine proteins (BSA, Hb and Cat) with different physical characteristics (**Table 1**) was determined using the prepared PS_{92}-*b*-P($HEMA_{63}$-*r*-$SEMA_{37}$)$_8^{150}$ membranes. The phosphate-buffered saline (PBS) having an ionic strength of 0.176 M was used to prepare protein solutions at pH 7.4. The retention of Cat and Hb was 97 % and 95 %, respectively, but only 20 % BSA was retained by the membrane (**Fig. 4**). Cat has a significantly larger size than BSA and the molecular weight is four-fold higher (**Table 1**). The ideal selectivity of BSA over Cat, $\psi_{BSA/Cat}$ was 27 (**Fig. 5**). However, $\psi_{Cat/Hb}$ was only 1.7 though the difference in molecular weight is similar for this protein pair. Moreover, $\psi_{BSA/Hb}$ was 16 in spite of the identical molecular weight of BSA and Hb. At pH 7.4 three of these proteins were on the alkaline side of their isoelectric point i.e. they acquired a net negative charge. [47] As the isoelectric point of Hb is 7.1 it is likely to possess a rather small net negative charge compared to BSA (isoelectric point 4.7) and Cat (isoelectric point 5.4) at pH 7.4 (**Table 1**). Therefore, it is clear that the excellent $\psi_{BSA/Hb}$ was not a result of electrostatic exclusion. If the electrostatic repulsion between the membrane and the proteins would be the dominating factor in determining the retention of the proteins the permeance of Hb would be higher than BSA through the carboxyl and hydroxyl group containing pores of the membrane. The obtained result

suggests the swelled pores of the membrane were small enough to effectively reject Hb. Thus, it is not surprising that the Cat was also effectively rejected by the membrane. The dimension of BSA (14 × 4 × 4 nm) resembles a prolate ellipsoid while that of Hb (7 × 5.5 × 5.5 nm) is more like a sphere. To enter the swelled pores of the membrane the ellipsoidal BSA can orient in a way that the long axis is perpendicular to the surface of the membrane. Such orientation is likely to minimize the hindrance of BSA permeation through the membrane, leading to the higher flux and lower retention of BSA. On the other hand, the probability of the sphere like Hb to enter the pores is significantly lower regardless of any orientation it takes. Thus, the excellent $\psi_{BSA/Hb}$ represents the shape selective nature of the soft P(HEMA$_{63}$-*r*-SEMA$_{37}$) pores of the membrane. Moreover, the hydrophilic amino acid content of BSA is higher than that of Hb (**Table 1**). It might have also facilitated the permeation of BSA through the hydrophilic pores of the PS$_{92}$-*b*-P(HEMA$_{63}$-*r*-SEMA$_{37}$)$_8^{150}$ membrane.

Table 1

Protein physical characteristics [48-50].

Characteristics	**Proteins**		
	Bovine serum albumin	**Hemoglobin**	**Catalase**
Source	Bovine serum	Bovine blood	Bovine liver
Molecular weight[a] [kDa]	66	65	250
Molecular size [nm]	14 × 4 × 4	7 × 5.5 × 5.5	9.7 × 9.2 × 6.7
Isoelectric point	4.7	7.1	5.4
Hydrophilic amino acid content (g / 100 g protein)	56.16	43.13	---
Protein charge at pH 7.4	-20.5	-4.0	---

[a] Suppliers data (Sigma-Aldrich)

To benchmark the separation efficiency of the prepared PS$_{92}$-*b*-P(HEMA$_{63}$-*r*-SEMA$_{37}$)$_8^{150}$ membrane we have investigated the single protein retention of 6 in-house prepared polyacrylonitrile (PAN) membranes, 11 commercial UF membranes having molecular weight cut-off between 100 ~ 500 kDa and 5 commercial isoporous membrane having nominal pore size 0.015 ~ 0.1 µm under similar condition (**Supporting Information, Section 7**). Among these membranes the isoporous anodisc having a nominal pore size of 0.02 µm has the lowest BSA retention (24 %) (**Fig. 4**). The BSA retention of the anodisc membrane was comparable with the prepared PS$_{92}$-*b*-P(HEMA$_{63}$-*r*-SEMA$_{37}$)$_8^{150}$ membrane. However, the retentions of Hb and Cat were 18% and 92%, respectively. The $\psi_{BSA/Cat}$ was 9.5 for the anodisc membrane owing to the size difference between BSA and Cat but the $\psi_{BSA/Hb}$ was only 0.9 (**Fig. 5**). In other words the anodisc membrane showed very good size selectivity but almost no shape selectivity. Similarly, the $\psi_{BSA/Cat}$ of the isoporous track-etched polycarbonate membranes having 0.05 and 0.08 µm nominal pore size were 21 and 20, respectively while the $\psi_{BSA/Hb}$ were 0.7 and 1, respectively. In general the track-etched polycarbonate membranes have very low porosities. Thus compared to the total surface area of the membrane the number of channels for the transport of the proteins is very low (**Supporting Information, Fig. S17**). During the retention measurement a very strong tendency of formation of a cake layer was observed

(**Supporting Information, Fig. S18, S19**). As a result the series of track-etched polycarbonate membranes having different nominal pore sizes did not show any systematic trend for the retention of different proteins with the increase of nominal pore size. For instance the retention properties of the membranes having 0.015 µm and 0.08 µm pores were almost identical though the pore size has more than 5 fold difference (**Fig. 4**). With an exception of the in-house prepared PAN-6 all the studied nonisoporous PAN, polyethersulfone, regenerated cellulose and polyvinylidene fluoride membranes had retentions above 90 % for BSA, Hb and Cat (**Fig. 4 and Supporting Information, Table S7**). The retention of BSA, Hb and Cat for the PAN-6 membrane were 55 %, 74 % and 99 %, respectively. PAN-6 had the highest $\psi_{BSA/Cat}$ = 41 among all the membranes studied here. However, the $\psi_{BSA/Hb}$ was only 1.7 for PAN-6. The PVDF_V5 had the highest BSA solution permeance of 52 ± 15 L m^{-2} h^{-1} bar^{-1} and $\psi_{BSA/Hb}$ = 5 (three fold lower than the PS_{92}-*b*-$P(HEMA_{63}$-*r*-$SEMA_{37})_8^{150}$ membrane) among all the in-house prepared PAN and the commercial membranes studied here. Similar values of $\psi_{BSA/Hb}$ were also reported in literature for isoporous PS-*b*-P4VP membranes at pH 7.4. Zhu *et al*. [6] reported a PS-*b*-P4VP isoporous SNIPS membrane which retained 86 % BSA and 97 % Hb from single protein aqueous solution which means $\psi_{BSA/Hb}$would be 4.7 (calculated by us for comparison with our data). Qiu *et al*. [5] reported a PS-*b*-P4VP isoporous SNIPS having a diffusion selectivity of ca. 6 for BSA over Hb at pH 7.4. The permeance of BSA and Hb solution through the prepared PS_{92}-*b*-$P(HEMA_{63}$-*r*-$SEMA_{37})_8^{150}$ membrane was 183 ± 9 L m^{-2} h^{-1} bar^{-1} and 32 ± 2 L m^{-2} h^{-1} bar^{-1}, respectively, which were higher than all other membranes studied here. To the best of our knowledge a combination of such high permeance of BSA and Hb solutions with a $\psi_{BSA/Hb}$ = 16 has never been reported before.

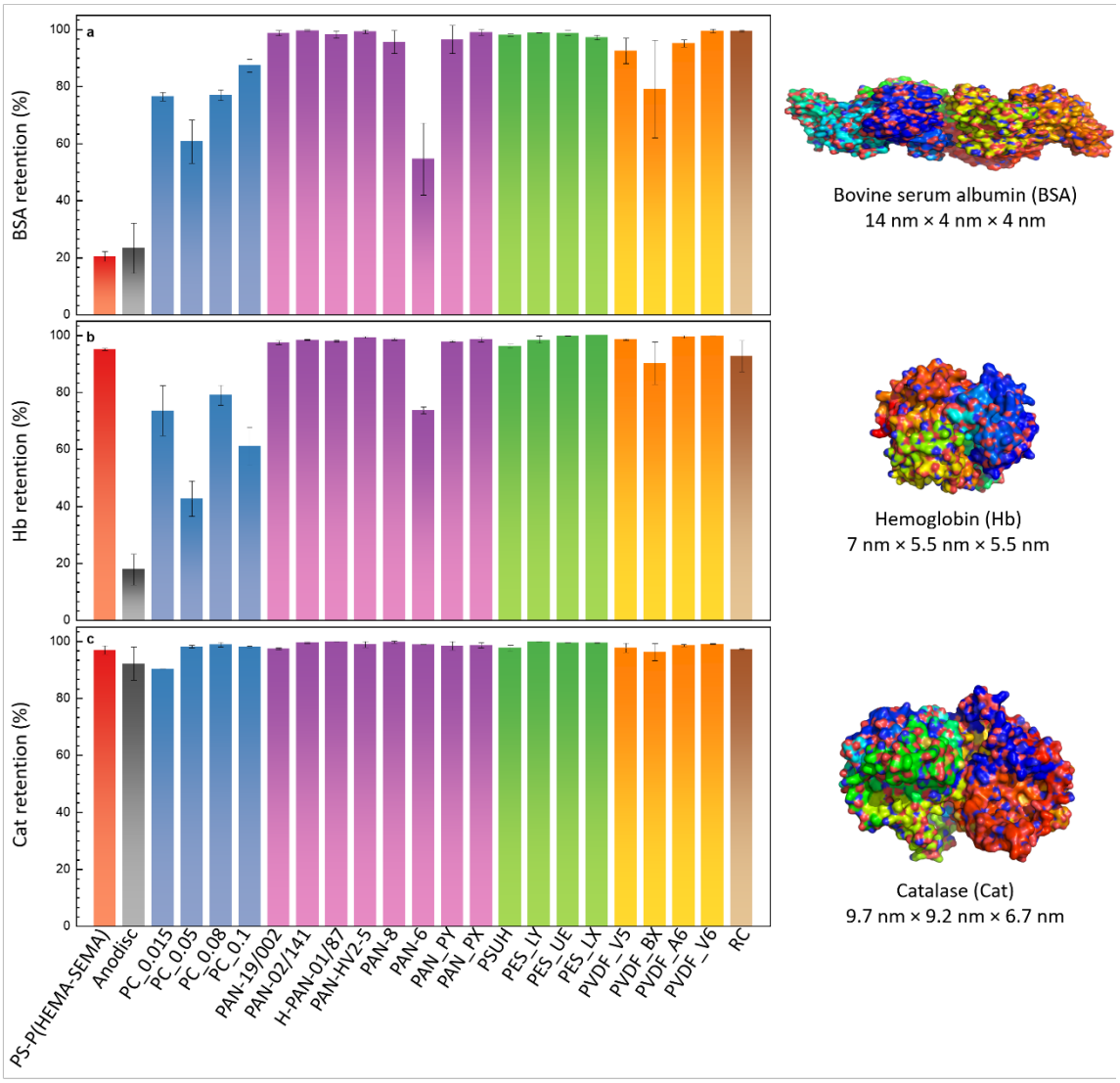

Fig. 4. a) BSA, b) Hb and c) Cat retentions of PS-*b*-P(HEMA-*r*-SEMA) and the traditional membranes in 1 g L^{-1} feed solution at pH 7.4.

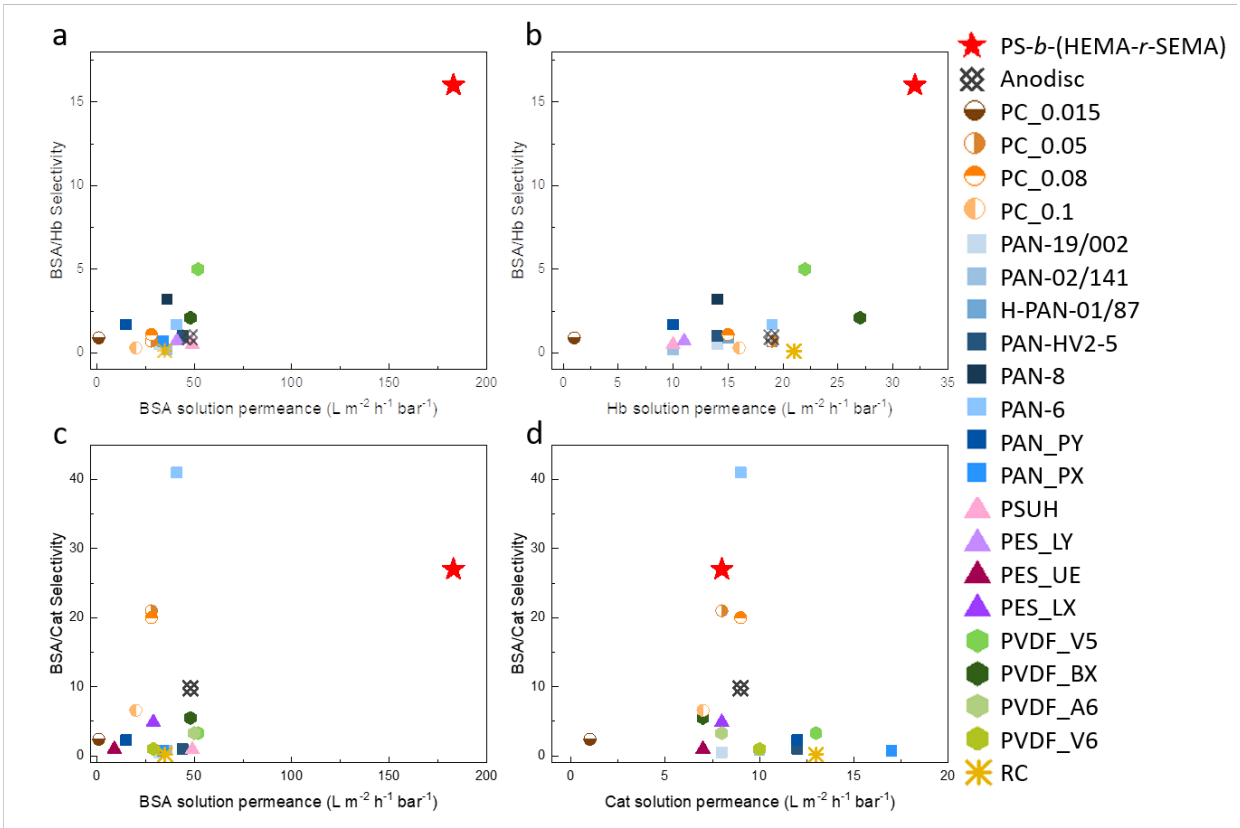

Fig. 5. The ideal selectivity of a) BSA/Hb as a function of BSA solution permeance; b) BSA/Hb as a function of Hb solution permeance; c) BSA/Cat as a function of BSA solution permeance; d) BSA/Cat as a function of Cat solution permeance for PS-*b*-P(HEMA-*r*-SEMA) and the traditional UF membranes. In some cases it was not possible to calculate the selectivity as the retention was close to 100%.

4. Conclusion

In this work we synthesized PS_{94}-*b*-$PHEMA_6^{149}$ via anionic polymerization followed by esterification with succinic anhydride to obtain a PS_{92}-*b*-$P(HEMA_{63}$-*r*-$SEMA_{37})_8^{150}$. Using this polymer we prepared an integral asymmetric isoporous membrane having randomly distributed hydroxyl and carboxyl groups along the pore walls in a one-step SNIPS method. The BSA selectivity of the PS_{92}-*b*-$P(HEMA_{63}$-*r*-$SEMA_{37})_8^{150}$ membrane over Hb and Cat was benchmarked with 22 commercial and in-house prepared membrane at pH 7.4 where three of the proteins had a net negative charge. The permeance of BSA solution through the PS_{92}-*b*-$P(HEMA_{63}$-*r*-$SEMA_{37})_8^{150}$ membrane was exceptionally higher than all the membranes studied here. Owing to four-fold higher molecular weight the permeation of Cat lagged far behind that of BSA which resulted in a $\psi_{BSA/Cat}$ = 27. The fair comparative study presented in this work showed a polyacrylonitrile membrane prepared by conventional nonsolvent induced phase separation had a better selectivity for this protein pair in spite of a large pore size distribution at the surface of the membrane. Moreover, the selectivity of two commercial isoporous membranes were comparable to the PS_{92}-*b*-$P(HEMA_{63}$-*r*-$SEMA_{37})_8^{150}$ membrane. Hence, despite the excellent BSA selectivity the prepared isoporous membrane does not offer a significant advantage over the membranes fabricated by conventional techniques for the separation of BSA from a protein which has significantly higher molecular weight. However, none of these conventional membranes matches the efficiency of the PS_{92}-*b*-$P(HEMA_{63}$-*r*-$SEMA_{37})_8^{150}$ membrane to separate BSA from Hb due to their identical molecular weight. By

taking advantage of the difference in shape and hydrophilicity of these proteins the PS_{92}-*b*-$P(HEMA_{63}$-*r*-$SEMA_{37})_8^{150}$ membrane allowed the BSA to pass through while blocking the permeation of Hb which resulted in a $\psi_{BSA/Hb}$ = 16. This unprecedented ideal selectivity of BSA over Hb at pH 7.4 is the greatest achievement of this work. Using the membranes prepared from conventional techniques such efficient separation of this protein pair is only possible at the isoelectric point of one of the proteins. Here we have demonstrated the potential of designing a membrane with functional isoporous channels to perform the separation without relying on the electroneutrality of one protein. In the last decade the scalable one-step SNIPS method has been recognized as a potential candidate to prepare next generation membranes having sharp molecular weight cut-off. With this work the SNIPS technique made a distinct progress and set up a new benchmark to prepare BSA selective isoporous membranes.

Acknowledgements

The authors thank Anke-Lisa Höhme, Erik Schneider, Silvio Neumann, Thomas Emmler, Maren Brinkmann and Petra Merten for characterizations of the block copolymer and membranes, Barbara Bajer for a big part of the flux and retention measurmenets, and Brigitte Lademann, Jan Wind and Berthold Wendland for technical support.

References

1. R. H. C. M. van Eijndhoven, S. Saksena, A. L. Zydney, Protein fractionation using electrostatic interactions in membranel filtration. Biotechnol. Bioeng. 48 (1995) 406-414. https://doi.org/10.1002/bit.260480413
2. R.-C. Hsiao, C.-L. Hung, S.-H. Lin, R.-S. Juang, Separation and flux characteristics in cross-flow ultrafiltration of bovine serum albumin and bovine hemoglobin solutions. Membr. Water. Treat. 2 (2011) 91-103. https://doi.org/10.12989/mwt.2011.2.2.091
3. D. A. Musale, S. S. Kulkarni, Relative rates of protein transmission through poly(acrylonitrile) based ultrafiltration membranes. J. Membr. Sci. 136 (1997) 13-23. https://doi.org/10.1016/S0376-7388(97)00179-8
4. R. Shukla, M. Balakrishnan, G. P. Agarwal, Bovine serum albumin-hemoglobin fractionation: significance of ultrafiltration system and feed solution characteristics. Bioseparation. 9 (2000) 7-19. https://doi.org/10.1023/A:1008194300403
5. X. Qiu, H. Yu, M. Karunakaran, N. Pradeep, S. P. Nunes, K.-V. Peinemann, Selective separation of similarly sized proteins with tunable nanoporous block copolymer membranes. ACS Nano. 7 (2013) 768-776. https://doi.org/10.1021/nn305073e
6. G.-D. Zhu, Y.-R. Ying, X. Li, Y. Liu, C.-Y. Yang, Z. Yi, C.-J. Gao, Isoporous membranes with sub-10 nm pores prepared from supramolecular interaction facilitated block copolymer assembly and application for protein separation. J. Membr. Sci. 566 (2018) 25-34.https://doi.org/10.1016/j.memsci.2018.08.033
7. H. Yu, X. Qiu, S. P. Nunes, K.-V. Peinemann, Biomimetic block copolymer particles with gated nanopores and ultrahigh protein sorption capacity. Nat. comm. 5 (2014) 4110. https://doi.org/10.1038/ncomms5110
8. R. Shevate, M. Kumar, H. Cheng, P.-Y. Hong, A. R. Behzad, D. Anjum, K.-V. Peinemann, Rapid size-based protein discrimination inside hybrid isoporous membranes. ACS Appl. Mater. Interfaces. 11 (2019) 8507-8516. https://doi.org/10.1021/acsami.8b20802
9. K.-V. Peinemann, V. Abetz, P. F. W. Simon, Asymmetric superstructure formed in a block copolymer via phase separation. Nat. Mater. 6 (2007) 992-996. https://doi.org/10.1038/nmat2038
10. A. Jung, S. Rangou, C. Abetz, V. Filiz, V. Abetz, Structure formation of integral asymmetric composite membranes of polystyrene-*block*-poly(2-vinylpyridine) on a nonwoven. Macromol. Mater. Eng. 297 (2012) 790-798. https://doi.org/10.1002/mame.201100359
11. C. Stegelmeier, V. Filiz, V. Abetz, J. Perlich, A. Fery, P. Ruckdeschel, S. Rosenfeldt, S. Förster, Topological paths and transient morphologies during formation of mesoporous block copolymer membranes. Macromolecules. 47 (2014) 5566-5577. https://doi.org/10.1021/ma5004908

12. M. Karunakaran, R. Shevate, K.-V. Peinemann, Nanostructured double hydrophobic poly(styrene-*b*-methyl methacrylate) block copolymer membrane manufactured via a phase inversion technique. RSC Adv. 6 (2016) 29064-29071. https://doi.org/10.1039/c6ra02313d

13. A. Jung, V. Filiz, S. Rangou, K. Buhr, P. Merten, J. Hahn, J. Clodt, C. Abetz, V. Abetz, Formation of integral asymmetric membranes of AB diblock and ABC triblock copolymers by phase inversion. Macromol. Rapid Comm. 34 (2013) 610-615. https://doi.org/10.1002/marc.201200770

14. R. M. Dorin, W. A. Philip, H. Sai, J. Werner, M. Elimelech, U. Wiesner. Designing block copolymer architectures for targeted membrane performance. Polymer 55 (2014) 347-353. https://doi.org/10.1016/j.polymer.2013.09.038

15. V. Abetz, Isoporous block copolymer membranes. Macromol. Rapid Comm. 36 (2015) 10-22. https://doi.org/10.1002/marc.201400556

16. M. Radjabian, V. Abetz, Advanced porous polymer membranes from self-assembling block copolymers. Prog. Polym. Sci. (2020) https://doi.org/10.1016/j.progpolymsic.2020.101219

17. Z. Zhang, Md. M. Rahman, C. Abetz, B. Bajer, J. Wang, V. Abetz, Quaternization of a polystyrene-*block*-poly (4-vinylpyridine) isoporous membrane: an approach to tune the pore size and the charge density. Macromol. Rapid Comm. 40 (2019) 1800729. https://doi.org/10.1002/marc.201800729

18. D. M. Stevens, J. Y. Shu, M.Reichert, A. Roy, Next-generation nanoporous materials: progress and prospects for reverse osmosis and nanofiltration. Ind. Eng. Chem. Res. 56 (2017) 10526-10551. https://doi.org/10.1021/acs.iecr.7b02411

19. M.T. M. Pendergast, E. M. V. Hoek, A review of water treatment membrane nanotechnologies. Energ. Environ. Sci. 4 (2011) 1946-1971. https://doi.org/10.1039/c0ee00541j

20. J. R. Werber, C. O. Osuji M. Elimelech, Materials for next-generation desalination and water purification membranes. Nat. Rev. Mater. 1 (2016) 16018. https://doi.org/10.1038/natrevmats.2016.37

21. E. A. Jackson, M. A. Hillmyer, Nanoporous membranes derived from block copolymers: from drug delivery to water filtration. ACS nano. 4 (2010) 3548-3553. https://doi.org/10.1021/nn1014006

22. Y. Zhang, J. L. Sargent, B. W. Boudouris, W. A. Phillip, Nanoporous membranes generated from self-assembled block polymer precursors: Quo Vadis? J. Appl. Polym. Sci. 132 (2015). https://doi.org/10.1002/app.41683

23. S. P. Nunes, Block copolymer membranes for aqueous solution applications. Macromolecules. 49 (2016) 2905-2916. https://doi.org/10.1021/acs.macromol.5b02579

24. J. Hahn, J. I. Clodt, V.Filiz, V. Abetz, Protein separation performance of self-assembled block copolymer membranes. RSC Adv. 4 (2014) 10252-10260.

https://doi.org/10.1039/c3ra47306f
25. J. I. Clodt, B. Bajer, K. Buhr, J. Hahn, V. Filiz, V. Abetz, Performance study of isoporous membranes with tailored pore sizes. J. Mem. Sci. 495 (2015) 334-340. https://doi.org/10.1016/j.memsci.2015.07.041
26. W. A. Phillip, R. M. Dorin, J. Werner, E. M. V. Hoek, U. Wiesner, M. Elimelech, Tuning structure and properties of graded triblock terpolymer-based mesoporous and hybrid films. Nano letters 11 (2011) 2892-2900. https://doi.org/10.1021/nl2013554
27. C. Höhme, J. Hahn, B. Lademann, A. Meyer, B. Bajer, C. Abetz, V. Filiz, V. Abetz, Formation of high thermally stable isoporous integral asymmetric block copolymer membranes. Eur. Polym. J. 85 (2016) 72-81. https://doi.org/10.1016/j.eurpolymj.2016.10.014
28. J. Hahn, V. Filiz, S. Rangou, B. Lademann, K. Buhr, J. I. Clodt, A. Jung, C. Abetz, V. Abetz, P*t*BS-*b*-P4VP and PTMSS-*b*-P4VP isoporous integral-asymmetric membranes with high thermal and chemical stability. Macromol. Mater. Eng. 298 (2013) 1315-1321. https://doi.org/10.1002/mame.201300012
29. D. Keskin, J. I. Clodt, J.Hahn, V. Abetz, V. Filiz, Postmodification of PS-*b*-P4VP diblock copolymer membranes by ARGET ATRP. Langmuir 30 (2014) 8907-8914. https://doi.org/10.1021/la501478s
30. C. Höhme, V. Filiz, C. Abetz, P. Georgopanos, N. Scharnagl, V. Abetz, Postfunctionalization of nanoporous block copolymer membranes via click reaction on polydopamine for liquid phase separation. ACS Appl. Nano Mater. 1 (2018) 3124-3136. https://doi.org/10.1021/acsanm.8b00289
31. J. I. Clodt, V. Filiz, S. Rangou, K. Buhr, C. Abetz, D. Höche, J. Hahn, A. Jung, V. Abetz, Double stimuli-responsive isoporous membranes via post-modification of pH-sensitive self-assembled diblock copolymer membranes. Adv. Funct. Mater. 23 (2013) 731-738. https://doi.org/10.1002/adfm.201370028
32. Y. Gu, U. Wiesner, Tailoring pore size of graded mesoporous block copolymer membranes: moving from ultrafiltration toward nanofiltration. Macromolecules. 48 (2015) 6153-6159. https://doi.org/10.1021/acs.macromol.5b01296
33. S. Rangou, K. Buhr, V. Filiz, J. I. Clodt, B. Lademann, J. Hahn, A. Jung, V. Abetz, Self-organized isoporous membranes with tailored pore sizes. J. Mem. Sci. 451 (2014) 266-275. https://doi.org/10.1016/j.memsci.2013.10.015
34. M. Radjabian, V. Abetz, Tailored pore sizes in integral asymmetric membranes formed by blends of block copolymers. Adv. Mater. 27 (2015) 352-355. https://doi.org/10.1002/adma.201404309
35. J. Wang, M. M. Rahman, C. Abetz, S. Rangou, Z. Zhang, V. Abetz, Novel post-treatment approaches to tailor the pore size of PS-*b*-PHEMA isoporous membranes. Macromol. Rapid Comm. 39 (2018) 1800435. https://doi.org/10.1002/marc.201800435

36. H. Yu, X. Qiu, S. P. Nunes, K. V. Peinemann, Self-assembled isoporous block copolymer membranes with tuned pore sizes. Angew. Chem. Int. Ed. 53 (2014) 10072-10076.
https://doi.org/10.1002/ange.201404491

37. S. Saleem, S. Rangou, C. Abetz, B. Lademann, V. Filiz, V. Abetz, Block copolymer membranes from polystyrene-*b*-poly(solketal methacrylate) (PS-*b*-PSMA) and amphiphilic polystyrene-*b*-poly(glyceryl methacrylate) (PS-*b*-PGMA). Polymers 9 (2017) 216.
https://doi.org/10.3390/polym9060216

38. S. Schöttner, H.-J. Schaffrath, M. Gallei, Poly(2-hydroxyethyl methacrylate)-based amphiphilic block copolymers for high water flux membranes and ceramic templates. Macromolecules 49 (2016) 7286-7295.
https://doi.org/10.1021/acs.macromol.6b01803

39. A. Hirao, H. Kato, K. Yamaguchi, S. Nakahama, Polymerization of monomers containing functional groups protected by trialkylsilyl groups. 5. Synthesis of poly (2-hydroxyethyl methacrylate) with a narrow molecular weight distribution by means of anionic living polymerization. Macromolecules 19 (1986) 1294-1299.
https://doi.org/10.1021/ma00159a002

40. X. Bories-Azeau, S. P. Armes, H. J. van den Haak, Facile synthesis of zwitterionic diblock copolymers without protecting group chemistry. Macromolecules 37 (2004) 2348-2352.
https://doi.org/10.1021/ma035904u

41. R. Ghosh, Z. Cui, Fractionation of BSA and lysozyme using ultrafiltration: effect of pH and membrane pretreatment. J. Mem. Sci. 139 (1998) 17-28.
https://doi.org/10.1016/S0376-7388(97)00236-6

42. S. P. Nunes, M. Karunakaran, N. Pradeep, A. R. Behzad, B. Hooghan, R. Sougrat, H. He, K.-V. Peinemann, From micelle supramolecular assemblies in selective solvents to isoporous membranes. Langmuir 27 (2011)10184-10190.
https://doi.org/10.1021/la201439p

43. M. Gallei, S. Rangou, V. Filiz, K. Buhr, S. Bolmer, C. Abetz, V. Abetz, The influence of magnesium acetate on the structure formation of polystyrene-*block*-poly(4-vinylpyridine)-based integral-asymmetric membranes. Macromol. Chem. Phys. 214 (2013) 1037-1046
https://doi.org/10.1002/macp.201200708

44. J. I. Clodt, S. Rangou, A. Schröder, K. Buhr, J. Hahn, A. Jung, V. Filiz, V. Abetz, Carbohydrates as additives for the formation of isoporous PS-*b*-P4VP diblock copolymer membranes. Macromol. Rapid Comm. 34 (2013) 190-194.
https://doi.org/10.1002/marc.201200680

45. P. Madhavan, K.-V. Peinemann, S. P. Nunes, Complexation-tailored morphology of asymmetric block copolymer membranes. ACS Appl. Mater. Interfaces 5 (2013) 7152-7159
https://doi.org/10.1021/am401497m

46. G.-W. Jin, H. Kim, J.-H. Seo, J. Ham, J.-S. Park, Y. Lee, Formation of polyion complex micelles with tunable isoelectric points based on zwitterionic block copolymers. Macromol. Res. 20 (2012) 1249-1256.

https://doi.org/10.1007/s13233-012-0177-0

47. C. Causserand, Y. Kara, P. Aimar, Protein fractionation using selective adsorption on clay surface before filtration. J. Mem. Sci. 186 (2001) 165-181. https://doi.org/10.1016/s0376-7388(01)00332-5

48. S. P. Palecek, A. L. Zydney, Hydraulic permeability of protein deposits formed during microfiltration: effect of solution pH and ionic strength. J. Mem. Sci. 95 (1994) 71-81. https://doi.org/10.1016/0376-7388(94)85030-5

49. H. P. Erickson, Size and shape of protein molecules at the nanometer level determined by sedimentation, gel filtration, and electron microscopy. Biol. Proced. Online 11 (2009) 32. https://doi.org/10.1088/2053-2563/ab19bach1

50. T. Samejima, M. Kamata, K. Shibata, Dissociation of bovine liver catalase at low pH. J. Biochem. 51 (1962) 181-187. https://doi.org/10.1093/oxfordjournals.jbchem.a127518

Supporting Information

Bovine serum albumin selective integral asymmetric isoporous membrane

Jiali Wang[1], Md. Mushfequr Rahman[1], Clarissa Abetz[1], Volker Abetz[1,2]*

[1]Helmholtz-Zentrum Geesthacht, Institute of Polymer Research, Max-Planck-Str. 1, 21502 Geesthacht, Germany

[2]Universität Hamburg, Institute of Physical Chemistry, Martin-Luther-King-Platz 6, 20146 Hamburg, Germany

*Corresponding author. Email address: volker.abetz@hzg.de

Content

Supporting Notes:

1. Reagents and membranes

Tetrahydrofuran (THF), N,N-dimethylformamide (DMF), 1,4-dioxane (DOX), *n*-hexane, hydrochloric acid fuming 37% (HCl) and methanol were ordered from Th. Geyer (Renningen, Germany) and Merck Millipore (Darmstadt, Germany). Styrene, 2-(trimethylsilyloxy)ethyl methacrylate (HEMA-TMS), lithium chloride (LiCl), *sec*-butyl lithium (*sec*-BuLi) (1.4 M in cyclohexane), di-*n*-butylmagnesium ($MgBu_2$) (1.0 M in heptane), 1,1-diphenylethylene (DPE), triethylaluminium (TEA) (1.0 M in hexane), calcium hydride (CaH_2), basic aluminum oxide, benzoic anhydride, succinic anhydride (SA), magnesium acetate ($MgAc_2$), coper acetate ($CuAc_2$), coper chloride (II) ($CuCl_2$) and proteins were purchased from Sigma-Aldrich (Schnelldorf, Germany). Deuterated solvents were purchased from Deutero GmbH (Kastellaun, Germany).

2. Synthesis of polystyrene-*block*-poly(2-hydroxyethyl methacrylate) (PS-*b*-PHEMA) diblock copolymer

Polystyrene-*block*-poly(2-(trimethylsilyloxy)ethyl methacrylate) (PS-*b*-P(HEMA-TMS)) was synthesized via sequential anionic polymerization of styrene and HEMA-TMS using Schlenk glasswares under an inert atmosphere of high vacuum (ca. 10^{-6} mbar, Edwards Germany GmbH, Munich, Germany) and argon supply (Argon 7.0, Linde AG, Pullach, Germany) following a protocol reported before (**Scheme S1**).[1, 2] THF was purified by successive distillation from *sec*-BuLi under argon atmosphere. Prior to use for the anionic polymerization, styrene was purified from basic aluminum oxide and freshly distilled from $MgBu_2$ under reduced pressure. HEMA-TMS was purified from basic aluminum oxide and stored over calcium hydride (CaH_2). HEMA-TMS was subsequently distilled under reduced pressure after treating twice with TEA before the anionic polymerization. The dried LiCl from a glovebox was suspended in the freshly distilled THF before initiation. The polymerization of styrene was initiated by *sec*-BuLi at -78 °C, and stirred for 2 h. An aliquot of polystyrene-precursor (PS-pre) was sampled out from the reactor and terminated with degassed methanol for further molecular characterization. Prior to addition of the second monomer, 1,1-diphenylethylene (DPE) was added to end-cap the polystyrene macroinitiator and the temperature was maintained at -30 °C for half an hour. The flask was then cooled down to −78 °C and HEMA-TMS was added via a syringe and the solution was stirred for further 3 h. The polymerization was quenched with degassed methanol. After concentrating the polymer solution by a rotary evaporator, the solution was precipitated into *n*-hexane to obtain the polymer. PS-*b*-PHEMA was obtained by cleavage of TMS group using concentrated hydrochloric acid. 1M HCl was added to the polymer in THF under continuous stirring at room temperature for 2 h, and then was precipitated in water, filtrated, and dried at 50 °C under vacuum until constant weight.

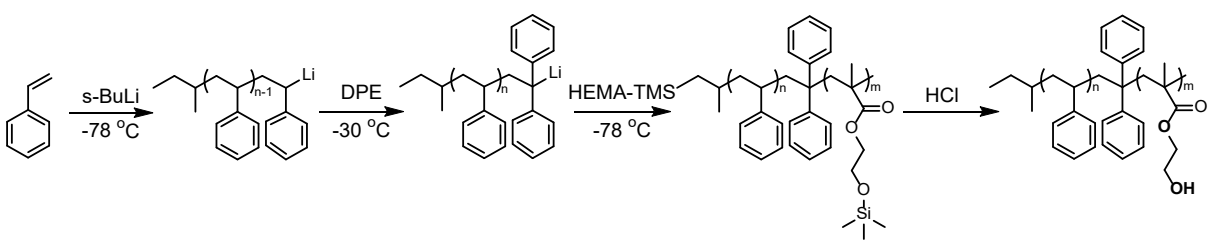

Scheme S1. Synthesis route of polystyrene-*block*-poly(2-hydroxyethyl methacrylate) (PS-*b*-PHEMA) block copolymer in tetrahydrofuran (THF) by sequential anionic polymerization of styrene and 2-(trimethylsilyloxy)ethyl methacrylate and subsequent hydrolysis.

3. Characterization of PS-*b*-PHEMA and benzoylated PS-*b*-PHEMA (PS-*b*-P(HEMA-Bz)) diblock copolymers by SEC and ^{1}H-NMR

To facilitate the characterization of PS-*b*-PHEMA block, the hydroxyl groups of the PHEMA segment were protected by benzoic anhydride (**Scheme S2**).[2] The characteristic peaks of polymers were quantitatively determined by proton nuclear magnetic resonance (^{1}H-NMR) (300 MHz, Bruker, Rheinstetten, Germany) using $CDCl_3$ and DMSO-d6 as solvents with internal standard tetramethylsilane (TMS). Dispersity index (Đ) and molecular weights of the PS-pre and the benzoylated PS-*b*-PHEMA (PS-*b*-P(HEMA-Bz)) diblock copolymers were determined by size exclusion chromatography (SEC). The measurements were performed at 25 °C in THF using 5 µm PSS SDV gel columns at a flow rate of 1.0 mL min^{-1} (VWR-Hitachi 1110 pump, Hitachi, Darmstadt, Germany). A Chromaster 5410 refractive-index detector (λ=254 nm) was used with a PS calibration. For the synthesized and discussed block copolymers, the subscripts denote the percentage weight fractions and the superscript the corresponding molecular weight of the block copolymer in kg mol^{-1}.

^{1}H-NMR spectra shows 100% conversion of benzoylation as shown in **Fig. S1**. According to the results calculated from SEC, the composition of PHEMA is 4 % (weight fraction) which is slightly lower than that calculated from ^{1}H-NMR by molar ratio (6%). Therefore, the molecular weight of the PHEMA block is calculated by the molecular weight of PS-precursor obtained from SEC in combination with the molar ratio of the PHEMA-Bz block to the PS block derived from ^{1}H-NMR in $CDCl_3$.

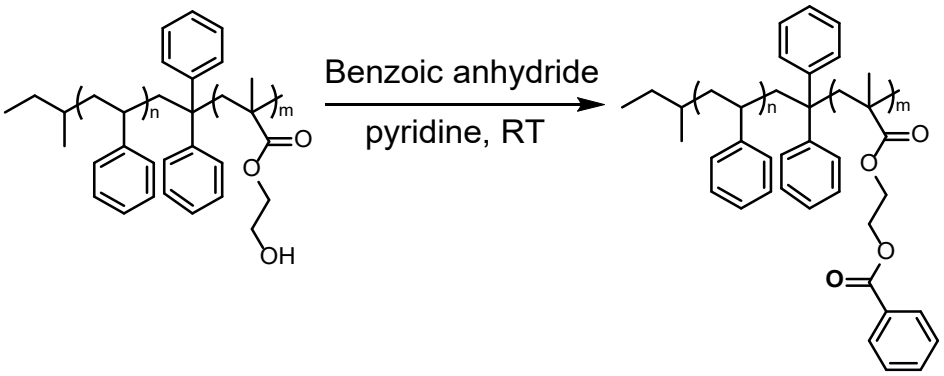

Scheme S2. Benzoylation of PS-*b*-PHEMA.

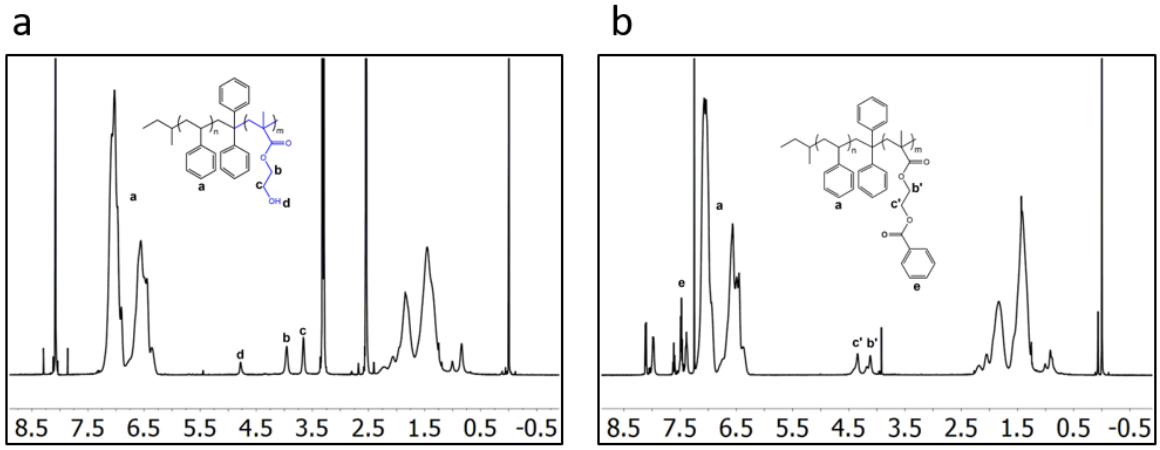

Fig. S1. ^{1}H-NMR spectra of (a) PS-*b*-PHEMA in $CDCl_3$ and DMSO-d6 (volume ratio of 1/1) and (b) PS-*b*-P(HEMA-Bz) in $CDCl_3$ with internal standard TMS.

Table S1. Characterization of PS-*b*-PHEMA and PS-*b*-P(HEMA-Bz) diblock copolymers by SEC with PS standard in THF.

Polymers [a]	**M_n** **[g mol^{-1}]**	**M_w** **[g mol^{-1}]**	***Đ***
PS-precursor	139 700	142 700	1.021
PS_{93}-*b*-P(HEMA-Bz)$_7$	159 100	212 100	1.059
PS_{96}-*b*-$PHEMA_4$ [b]	145 533	---	---
PS_{94}-*b*-$PHEMA_6$ [c]	148 617	---	---

[a] Subscripts indicate weight fraction (%) of the blocks.
[b] Molecular weight is calculated by equivalent molar ratio of PS-*b*-P(HEMA-Bz) from SEC.
[c] Molecular weight is calculated from ^{1}H-NMR in $CDCl_3$ and DMSO-d6 (volume ratio of 1/1) based on PS-precursor molecular weight from SEC;

4. Synthesis and characterization of polystyrene-*block*-poly(2-hydroxyethyl methacrylate-*ran*-2-(succinyloxy)ethyl methacrylate) (PS-*b*-P(HEMA-*r*-SEMA)) block copolymers

In a 250 mL round-bottomed flask PS-*b*-PHEMA diblock copolymer (5.00 g, 2.31 mmol OH residues) was dissolved in anhydrous pyridine (20 mL) at room temperature under argon. Under argon flow, succinic anhydride (1.15 g, 11.5 mmol) dissolved in anhydrous pyridine (1 mL) was added.[3] In order to control the degree of esterifaction the reaction time was varied between 2 ~ 240 hours. The reaction was terminated by adding 2 mL methanol and exposing to the air under ice bath for 20 min. The reaction mixture was precipitated into 200 mL of methanol to remove the excess succinic anhydride and obtain the polymer. The precipitate was redissolved in 10 mL of pyridine and precipitated into 100 mL of methanol twice to make sure no residues of reagents. The polymers were dried under vacuum at 50 °C until constant weight.

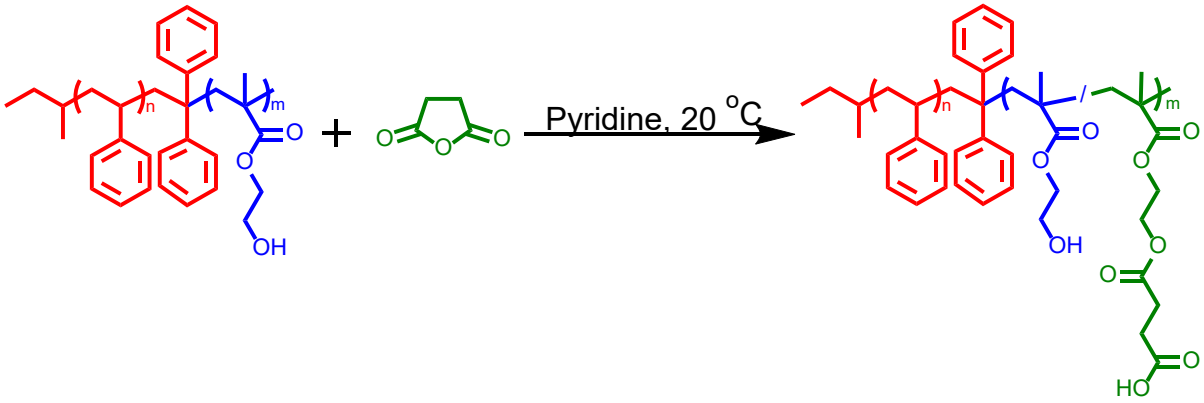

Scheme S3. Synthesis route of polystyrene-*block*-poly(2-hydroxyethyl methacrylate-*ran*-2-succinyloxyethyl methacrylate) (PS-*b*-P(HEMA-*r*-SEMA)) in pyridine at room temperature by the esterification of succinic anhydride.

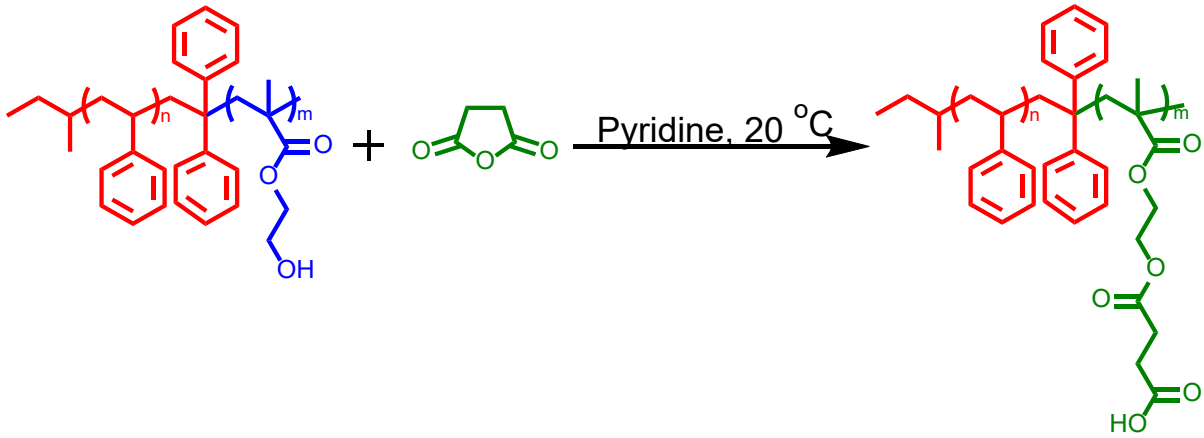

Scheme S4. Synthesis route of polystyrene-*block*-poly(2-succinyloxyethyl methacrylate) (PS-*b*-PSEMA) in pyridine at room temperature by the esterification of succinic anhydride.

Table S2 shows the molecular weight and composition of the prepared polymers determined by SEC and ^{1}H-NMR respectively. The ^{1}H-NMR spectrum of PS_{92}-*b*-P($HEMA_{63}$-*r*-$SEMA_{37}$)$_8^{150}$ is depicted in **Fig. S2**) as an example.

Table S2. Characterization of PS-*b*-PHEMA, PS-*b*-P(HEMA-*r*-SEMA), PS-*b*-SEMA polymers.

Polymers [a]	**Reaction time [h]**	**Content of PSEMA [wt %]** [b]	**Content of PS [wt %]** [c]	**PHEMA or P(HEMA-*r*-SEMA) or PSEMA [wt %]** [c]	**Total molecular weight [kg mol^{-1}]** [d]
PS_{94}-*b*-$PHEMA_6^{149}$	0	0	94	6	149
PS_{93}-*b*-P($HEMA_{95}$-*r*-$SEMA_5$)$_7^{149}$	2	5	93	7	149
PS_{92}-*b*-P($HEMA_{85}$-*r*-$SEMA_{15}$)$_8^{149}$	6	15	92	8	149
PS_{92}-*b*-P($HEMA_{63}$-*r*-$SEMA_{37}$)$_8^{150}$	60	37	92	8	150
PS_{90}-*b*-P($HEMA_{43}$-*r*-$SEMA_{57}$)$_{10}^{151}$	120	57	90	10	151

PS_{77}-*b*-$PSEMA_{23}^{155}$	240	100	77	23	155

[a] Subscripts indicate weight fraction (%) of the blocks; Superscripts indicate the molecular weight (kg mol^{-1}).
[b] Calculated by ^{1}H-NMR according to the molar ratios of PHEMA to PSEMA segments.
[c] Calculated by ^{1}H-NMR according to the molar ratios of PS segments to PHEMA and PSEMA segments;
[d] Determined by ^{1}H-NMR based on PS-precursor molecular weight from SEC;

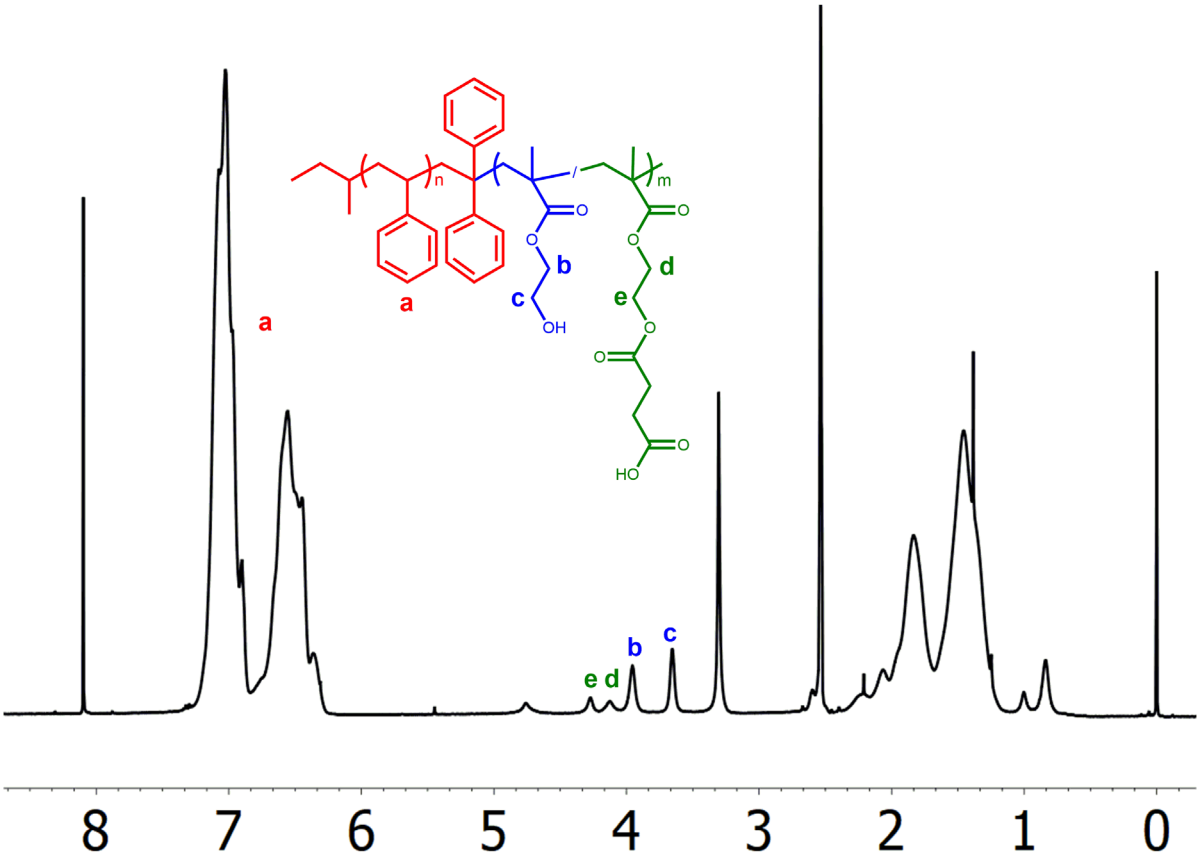

Fig. S2. ^{1}H-NMR spectra of PS_{92}-*b*-P($HEMA_{63}$-*r*-$SEMA_{37}$)$_8^{150}$ in $CDCl_3$ and DMSO-d6 (volume ratio of 1/1) with internal standard TMS.

5. Calculation of the solubility parameters of homopolymers

Solubility parameters of PS and solvents were reported by D.W. Van Krevelen et. al and C. M. Hansen.[4, 5] PHEMA solubility parameter was evaluated by Hou et al. using UV-vis spectroscope by comparing ultraviolet absorption intensity of different molecular weight samples in methanol, methanol/2-butanone (m/m=3:2 and 2:3) or 2-butanone.[6] For the solubility parameter of PSEMA no direct experimental data were found in the literature. Thus it was theoretically calculated by Hoy's method according to the **Equations S1-S9** for an amorphous polymer.[5]

$$\boldsymbol{F}_t = \sum N_i \boldsymbol{F}_{t,i} \quad (1)$$

$$\boldsymbol{V} = \sum N_i \boldsymbol{V}_i \quad (2)$$

$$\Delta_T{}^{(P)} = \sum N_i \Delta_{T,i}{}^{(P)} \quad (3)$$

$$\boldsymbol{\alpha^{(P)}} = \mathbf{777}\,\frac{\Delta_T{}^{(P)}}{\boldsymbol{V}} \quad (4)$$

$$\bar{n} = \frac{0.5}{\Delta_T{}^{(P)}} \quad (5)$$

$$\delta_t = \frac{\boldsymbol{F_t} + \frac{\boldsymbol{B}}{\bar{n}}}{\boldsymbol{V}} \quad (6)$$

$$\delta_p = \delta_t \sqrt{\frac{1}{\boldsymbol{\alpha^{(P)}}}\,\frac{\boldsymbol{F_p}}{\boldsymbol{F_t} + \frac{\boldsymbol{B}}{\bar{n}}}} \quad (7)$$

$$\delta_h = \delta_t \sqrt{\frac{\boldsymbol{\alpha^{(P)}} - \mathbf{1}}{\boldsymbol{\alpha^{(P)}}}} \quad (8)$$

$$\delta_d = \sqrt{{\delta_t}^2 - {\delta_p}^2 - {\delta_h}^2} \quad (9)$$

$\boldsymbol{F_t}$ is the molar attraction function; $\boldsymbol{V}$ is the molar volume of the structural unit of the polymer. Δ_T is the Lydersen correction for non-ideality, used in the auxiliary equations. The values for amorphous polymers $\Delta_T{}^{(P)}$ and $\boldsymbol{\alpha^{(P)}}$ were derived by Hoy. $\bar{n}$ is the number of repeating units per effective chain segment of the polymer. Note that $\boldsymbol{F_t}$ must always be combined with a Base value (**B**).

Table S3 gives values of increments in Hoy's system for the molar attraction function.

Table S3. Values of increments in Hoy's System (1985), for the molar attraction function[5]

Groups	$\boldsymbol{F_{t,i}}$ **[(MJ$^{0.5}$ m$^{-1.5}$ mol^{-1}]**	$\boldsymbol{F_{p,i}}$	$\Delta_{T,i}{}^{(P)}$	$\boldsymbol{V_i}$ **[cm^3 mol^{-1}]**
—CH_3	303.5	0	0.022	21.55
—CH_2—	269.0	0	0.020	15.55
>CH—	176.0	0	0.013	9.56
>C<	65.5	0	0.040	3.56
CH_{ar}	241	62.5	0.018	13.42
C_{ar}	201	65	0.015	7.42
—OH	675	675	0.049	12.45
—COOH	565	415	0.039	26.1

—COO—	640	528	0.050	23.7

Configurations	$F_{t,i}$ **[(MJ$^{0.5}$ m$^{-1.5}$ mol^{-1}]**	$\Delta_{T,i}^{(P)}$	V_i **[cm^3 mol^{-1}]**
Base value (**B**)	277	-	-

Table S4. Hansen Solubility parameters of solvents and homopolymers. [4-6]

Polymers/Solvents	δ **[MPa$^{0.5}$]**	δ_d **[MPa$^{0.5}$]**	δ_p **[MPa$^{0.5}$]**	δ_h **[MPa$^{0.5}$]**
PS	20.1	17.6	6.1	4.1
PHEMA	23.3	15.8	11.8	14.8
THF	19.5	16.8	5.7	8.0
DMF	24.9	17.4	13.7	11.3
DOX	20.5	19.0	1.8	7.4

Table S5. Hansen Solubility parameters of homopolymers calculated by Hoy's method. [5]

Polymers/Solvents	δ **[MPa$^{0.5}$]**	δ_d **[MPa$^{0.5}$]**	δ_p **[MPa$^{0.5}$]**	δ_h **[MPa$^{0.5}$]**
PS	19.3	16.7	8.3	5.1
PHEMA	24.2	14.1	13.0	14.8
PSEMA	21.1	14.3	11.5	10.5

Table S4 and **Table S5** show the experimentally determined and the theoretical values of the solubility parameters of the PS and PHEMA slightly deviate from each other. Compared to PHEMA the value of δ is lower for PSEMA which stems from the lower values to δ_p and δ_h. The theoretical values of δ of the P(HEMA-*r*-SEMA) segments of any composition are in the range 21.1 ~ 24.2 while that of δ_p are in the range 11.5 ~ 13.0. A comparison of the δ_p values of the solvents suggest for 6 synthesized polymers the nonpolar THF and DOX has more affinity for the PS block DMF has more affinity for the pore forming blocks of the membranes i.e. PHEMA, P(HEMA-*r*-SEMA) and PSEMA.

6. Fabrication of PS-*b*-P(HEMA-*r*-SEMA) copolymer membranes by SNIPS

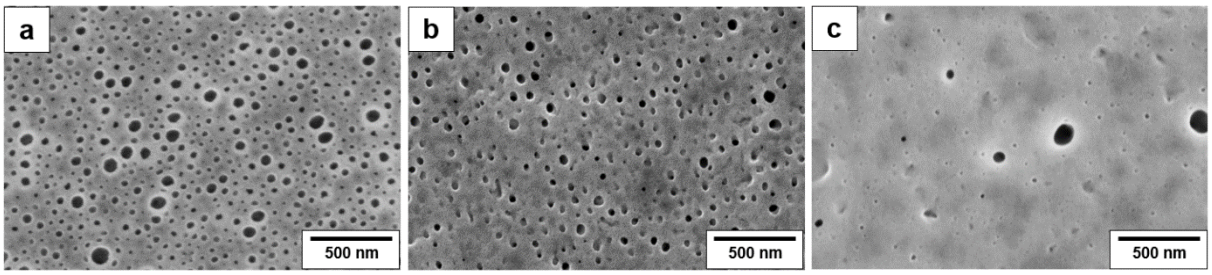

Fig. S3. SEM images of PS_{94}-*b*-$PHEMA_6^{149}$ membrane top surface in THF/DMF/DOX (2:1:1) a) 22 wt % casting solution at the evaporation time of 25 s; b) 18 wt % casting solution at the evaporation time of 10 s; c) 14 wt % casting solution at the evaporation time of 5 s.

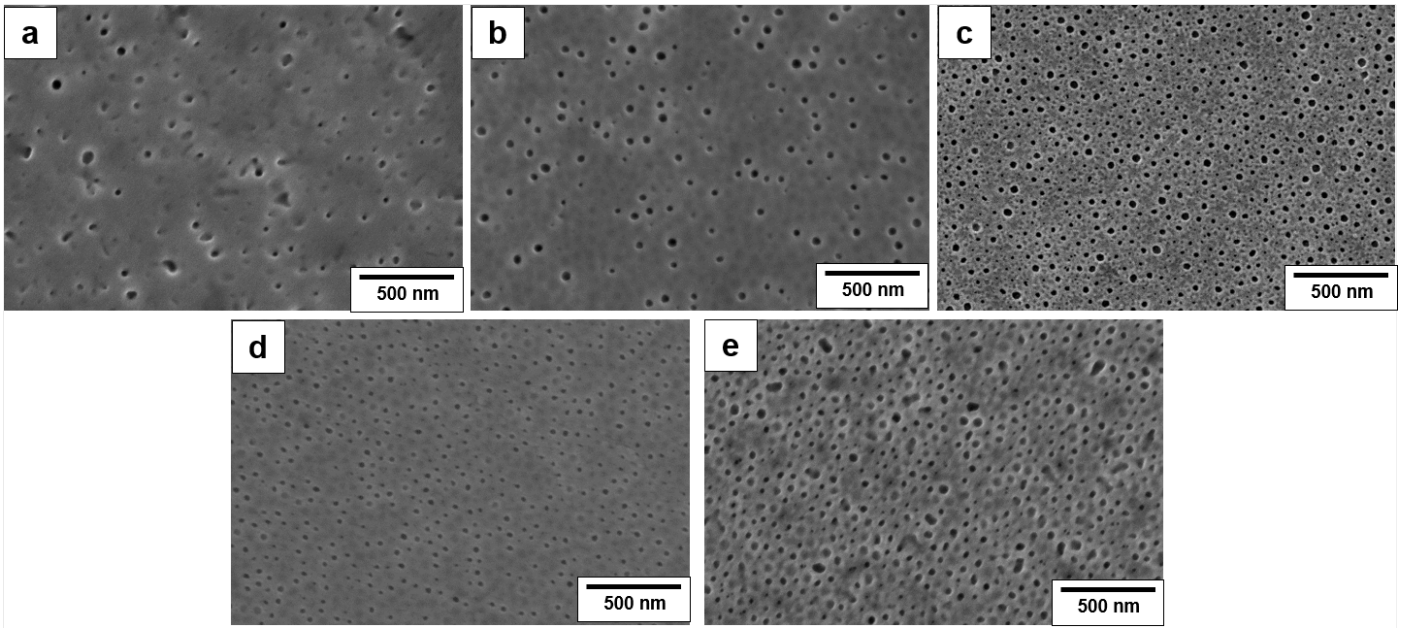

Fig. S4. SEM images of membrane top surface prepared from a) 21 wt % PS_{93}-*b*-P($HEMA_{95}$-*r*-$SEMA_5)_7^{149}$ casting solution in THF/DMF/DOX (2:1:1) at the evaporation time of 20 s ; b) 21 wt % PS_{92}-*b*-P($HEMA_{85}$-*r*-$SEMA_{15})_8^{149}$ casting solution in THF/DMF/DOX (2:1:1) at the evaporation time of 15 s; c) 22 wt % PS_{92}-*b*-P($HEMA_{63}$-*r*-$SEMA_{37})_8^{150}$ casting solution in THF/DMF/DOX (2:1:1) at the evaporation time of 25 s; d) 25 wt % PS_{90}-*b*-P($HEMA_{43}$-*r*-$SEMA_{57})_{10}^{151}$ casting solution in THF/DMF/DOX (2:1:1) at the evaporation time of 5 s; e) 20 wt % PS_{77}-*b*-$PSEMA_{23}^{155}$ casting solution in THF/DMF/DOX (2:1:1) at the evaporation time of 35 s.

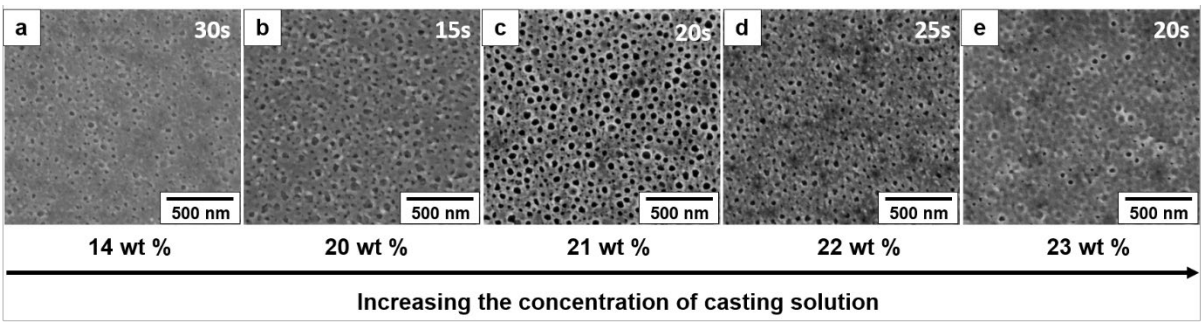

Fig. S5. SEM images of membrane top surface prepared from PS_{92}-*b*-P($HEMA_{63}$-*r*-$SEMA_{37}$)$_8^{150}$ with different concentrations of casting solution in THF/DMF/DOX (1:1:1) at the different evaporation times.

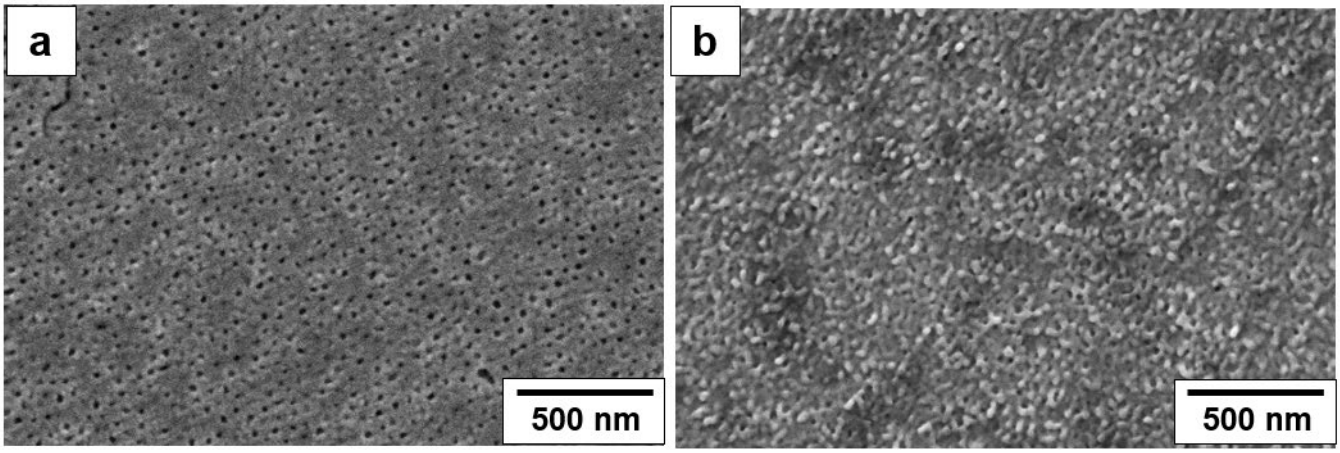

Fig. S6. SEM images of membrane top surface prepared from PS_{92}-*b*-P($HEMA_{63}$-*r*-$SEMA_{37}$)$_8^{150k}$ in THF/DMF/DOX (1:1:1). a) 20 wt % casting solution with 1.0 wt % $MgAc_2$ (viscosity 660 Pa s) at the evaporation time of 10 s; b) 21 wt % casting solution with 0.15 wt % $CuAc_2$ (viscosity 987 Pa s) at the evaporation time of 25 s.

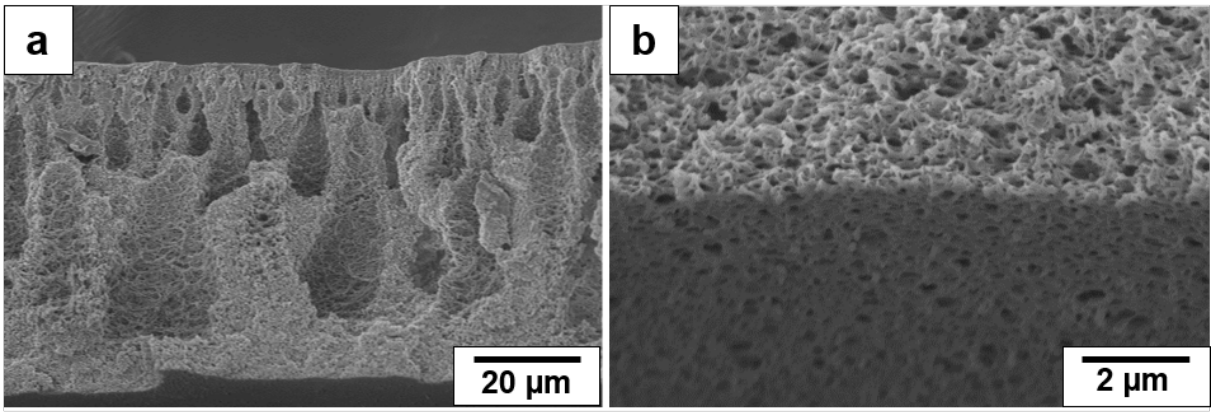

Fig. S7. SEM images of the cross-section of a) the overall membrane; b) the bottom surface prepared from 20 wt % PS_{92}-*b*-P($HEMA_{63}$-*r*-$SEMA_{37}$)$_8^{150k}$ casting solution in THF/DMF/DOX (1:1:1) with 0.1 wt % $MgAc_2$ at the evaporation time of 25 s which was casted on the nonwoven support.

7. Membrane performance

I. Specifications of membranes

Table S6. The features of the commercial and in-house prepared UF membranes

Membrane	NMWCO or NPZ [a]	Material	Company
Anodisc	0.02 µm	Aluminum oxide	Whatman
PC_0.015	0.015 µm	Polycarbonate	Whatman
PC_0.05	0.05 µm	Polycarbonate	Whatman

PC_0.08	0.08 µm	Polycarbonate	Whatman
PC_0.1	0.1 µm	Polycarbonate	Whatman
PAN-19/002	---	Polyacrylonitrile	In-house prepared [b]
PAN-02/141	---	Polyacrylonitrile	In-house prepared [b]
H-PAN-01/87	---	Polyacrylonitrile	In-house prepared [b]
PAN-HV2-5	---	Polyacrylonitrile	In-house prepared [b]
PAN-8	---	Polyacrylonitrile	In-house prepared [b]
PAN-6	---	Polyacrylonitrile	In-house prepared [b]
PSUH	100 kDa	Ultra-hydrophilic polysulfone	Sterlitech
PES_LY	100 kDa	Polyethersulfone	Sterlitech
PES_UE	100 kDa	Polyethersulfone	Sterlitech
PAN_PY	100 kDa	Polyacrylonitrile	Sterlitech
PVDF_V5	200 kDa	Positively charged polyvinylidene fluoride	Sterlitech
PVDF_BX	250 kDa	Polyvinylidene fluoride	Sterlitech
PES_LX	300 kDa	Polyethersulfone	Sterlitech
PAN_PX	300 kDa	Polyacrylonitrile	Sterlitech
RC	500 kDa	Regenerated cellulose	Sterlitech
PVDF_A6	500 kDa	Polyvinylidene fluoride	Sterlitech
PVDF_V6	500 kDa	Positively charged polyvinylidene fluoride	Sterlitech

[a] The commercial membranes were purchased from Sterlitech Co. (Washington, USA) with the nominal molecular weight cutoff (NMWCO) of 100 ~ 500 kDa and from Whatman (Pittsburgh, USA) with the nominal pore size (NPZ) of 0.015 ~ 0.1 µm.

[b] The PAN membranes were prepared by Helmholtz-Zentrum Geesthacht.

II. Pretreatment of the commercial membranes

All the membranes from Sterlitech Co. were pretreated to remove the protective layer throughout the membrane before membrane performance measurements. The membranes were soaked in 10 vol % ethanol aqueous solution for 10 min using the shaking bed at the speed of 90 rad/min. Subsequently, the membranes were washed with pure water at the trans-membrane pressure of 2 bar for 20 min until the water permeance is stable. The corresponding

membrane surface morphologies before and after pretreatment were investigated by SEM (**Fig. S8-S11**).

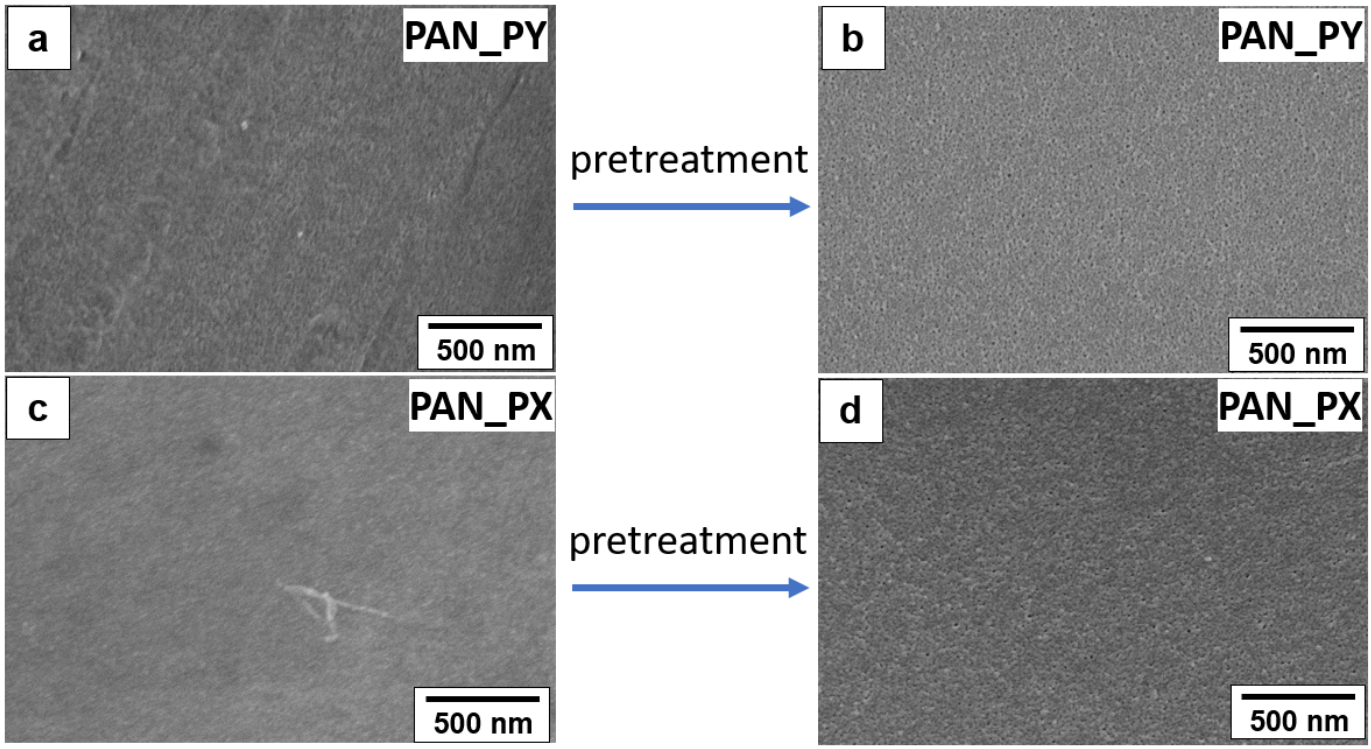

Fig. S8. SEM images of (a-b) PAN_PY and (c-d) PAN_PX membrane surfaces before and after pretreatment.

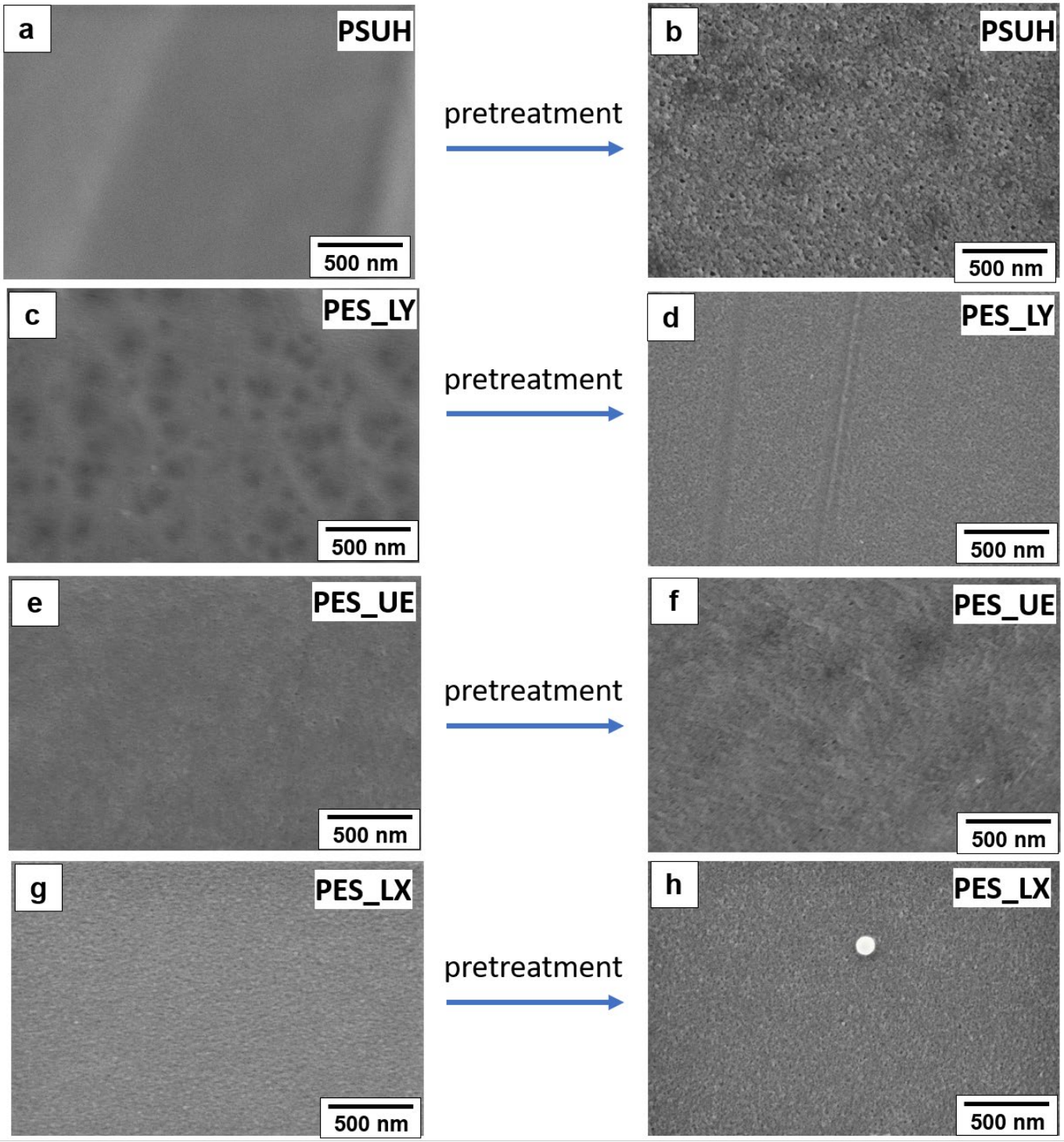

Fig. S9. SEM images of (a-b) PSUH, (c-d) PES_LY, (e-f) PES_UE and (g-h) PES_LX membrane surfaces before and after pretreatment.

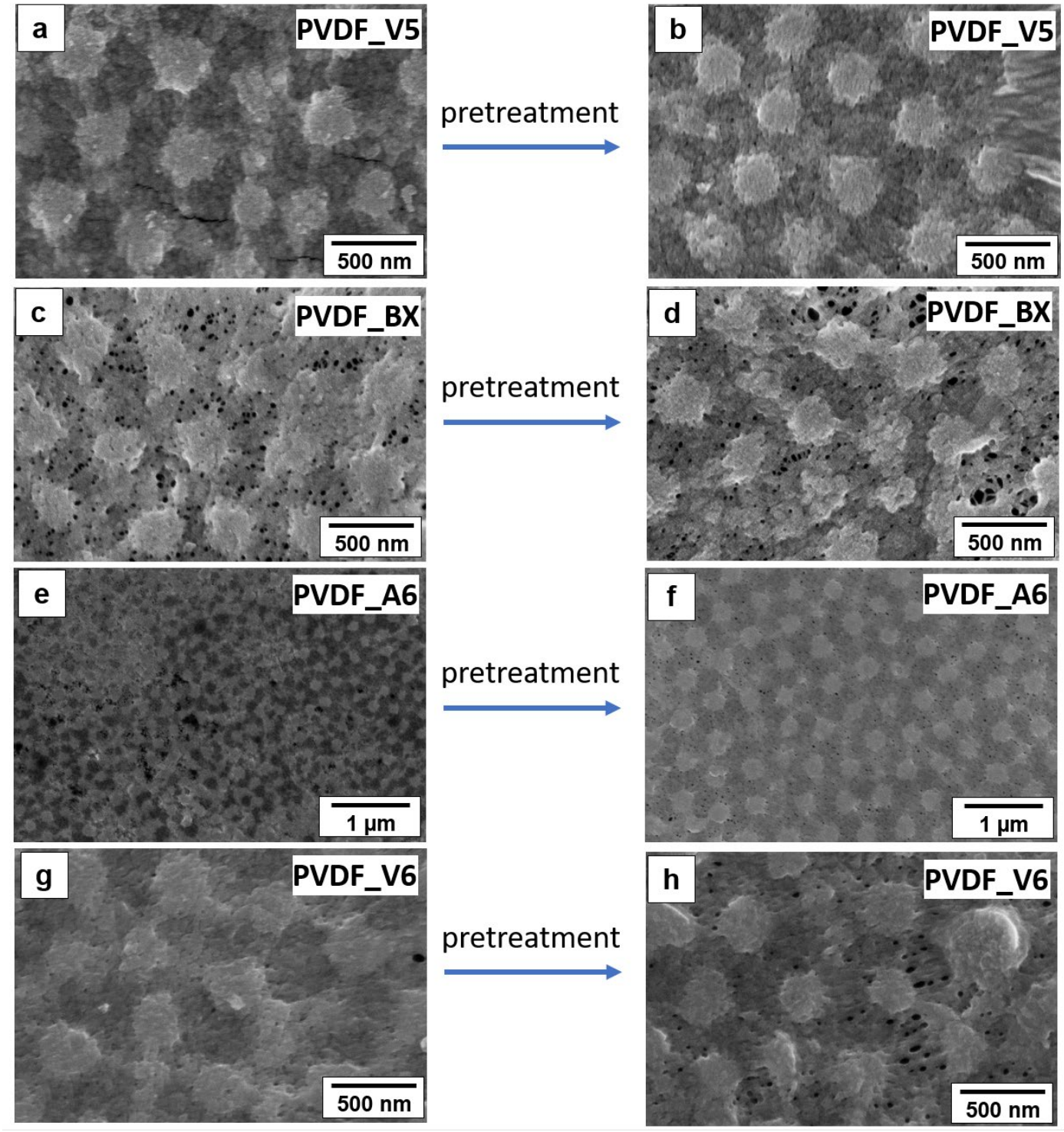

Fig. S10. SEM images of (a-b) PVDF_V5, (c-d) PVDF_BX, (e-f) PVDF_A6 and (g-h) PVDF_V6 membrane surfaces before and after pretreatment.

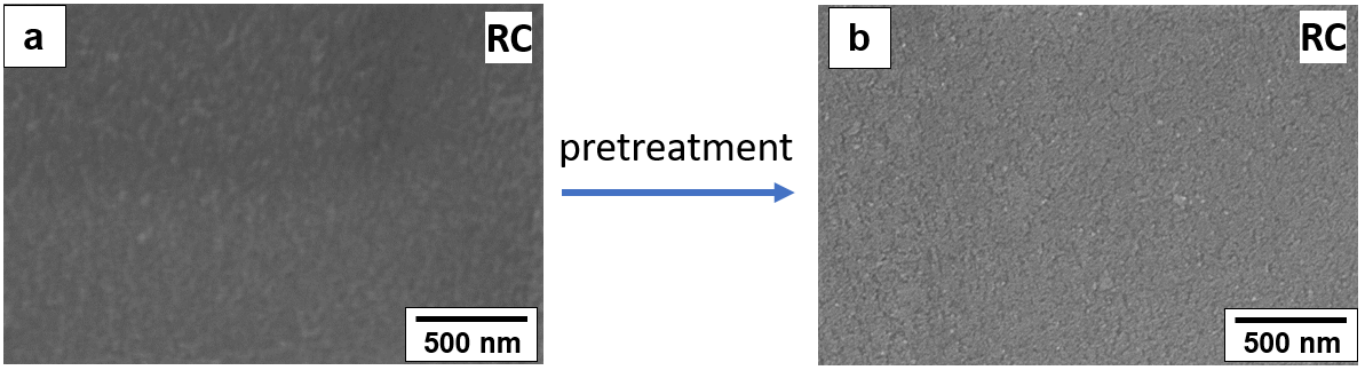

Fig. S11. SEM images of (a-b) RC membrane surfaces before and after pretreatment.

III. Pure water permeance measurements

The water permeance measurements were conducted in a dead-end mode at a constant feed pressure of 2 and 3 bar at 20 °C. The mean water permeance of PC_0.08, PC_0.1 and Anodisc within the first 1 hour at a constant feed pressure of 3 bar using the test unit as shown in **Fig. S14** and PAN-6 membranes within the first 1 hour and the rest of membranes within the first 7 hours at a constant feed pressure of 2 bar at 20 °C using the test unit as shown in **Fig. S12**. These studies were performed by using demineralized water which had an electrical conductivity of $\approx$ 0.055 µS cm^{-1}. The volume change of water permeance (ΔV) was measured gravimetrically over a balance every 60 sec and pressure was measured as well. The effective membrane area (A) was 1.77 cm^2. All the membranes were soaked in demineralized water for 24 h before measurement to ensure the sufficient swelling of membrane. All experiments were performed at least three times by using three individual samples.

The water permeance (J) is calculated as:

$$J = \frac{\Delta V}{A \cdot \Delta t \cdot \Delta p} \tag{10}$$

Where, ΔV is the volume change of water permeance between two mass measurements, A is the effective membrane area, Δt is the time interval between two mass measurements, Δp is the trans-membrane pressure.

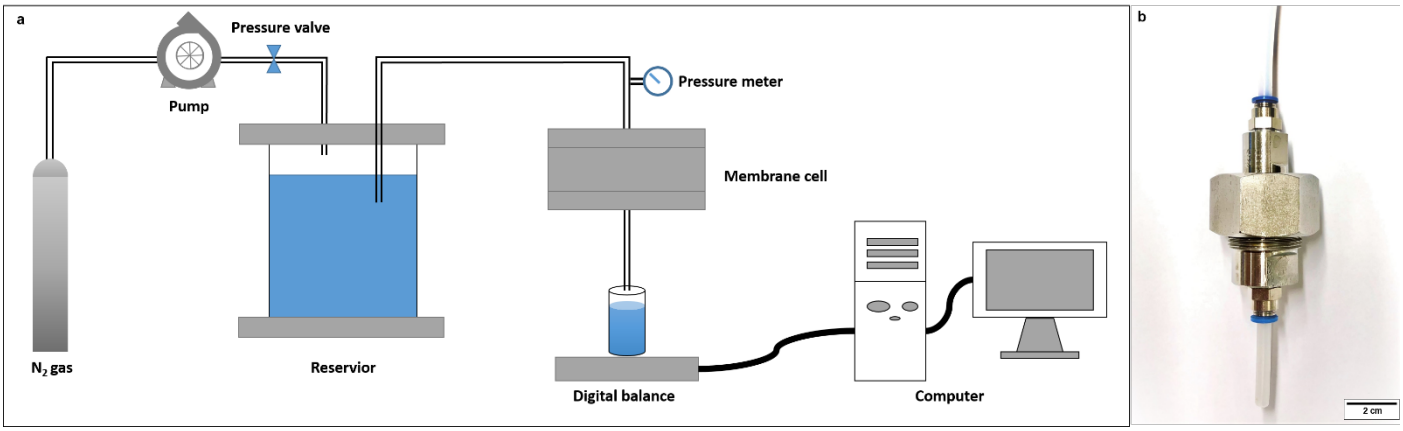

Fig. S12. a) Schematic representation of the experimental setup involving dead-end filtration system; b) membrane cell

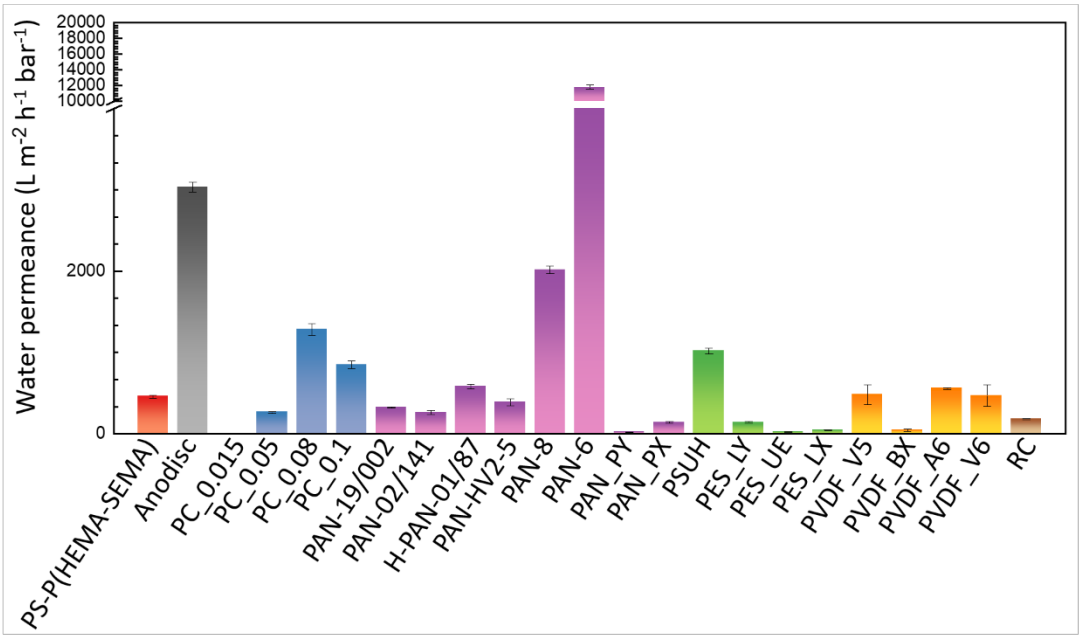

Fig. S13. The mean water permeance of PS-*b*-P(HEMA-*r*-SEMA) and the traditional membranes.

IV. Water permeance measurement as a function of pH

The water permeance measurements as a function of pH were performed in the pH range of 3 ~ 13 in a dead-end mode with continuously stirring at a trans-membrane pressure of 1 bar at 20 °C as shown in **Fig. S14**. The membrane testing cell is purchased from EMD Millipore™ and refitted to our house-made devices. The effective membrane area was 1.77 cm^2. The volume change of permeance (ΔV) was measured gravimetrically over a balance every 60 sec and pressure was measured as well. Permeancees at each pH value were measured for 20 min and calculated the average value. All the membranes were soaked in demineralized water for 24 h before measurement to ensure the sufficient swelling of membrane. Each measurement was conducted three times using three individual samples.

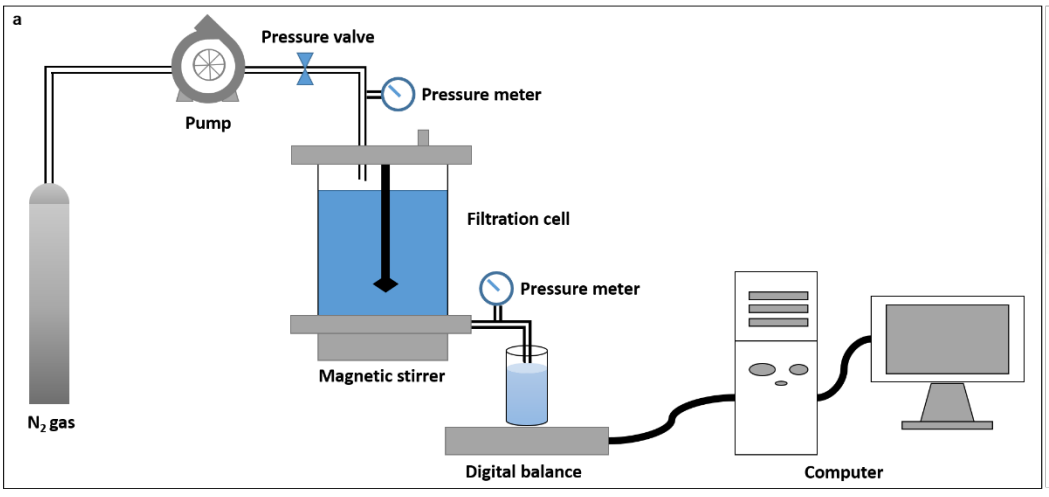

Fig. S14. a) Schematic representation of the experimental setup involving dead-end filtration system; b) membrane filtration cell

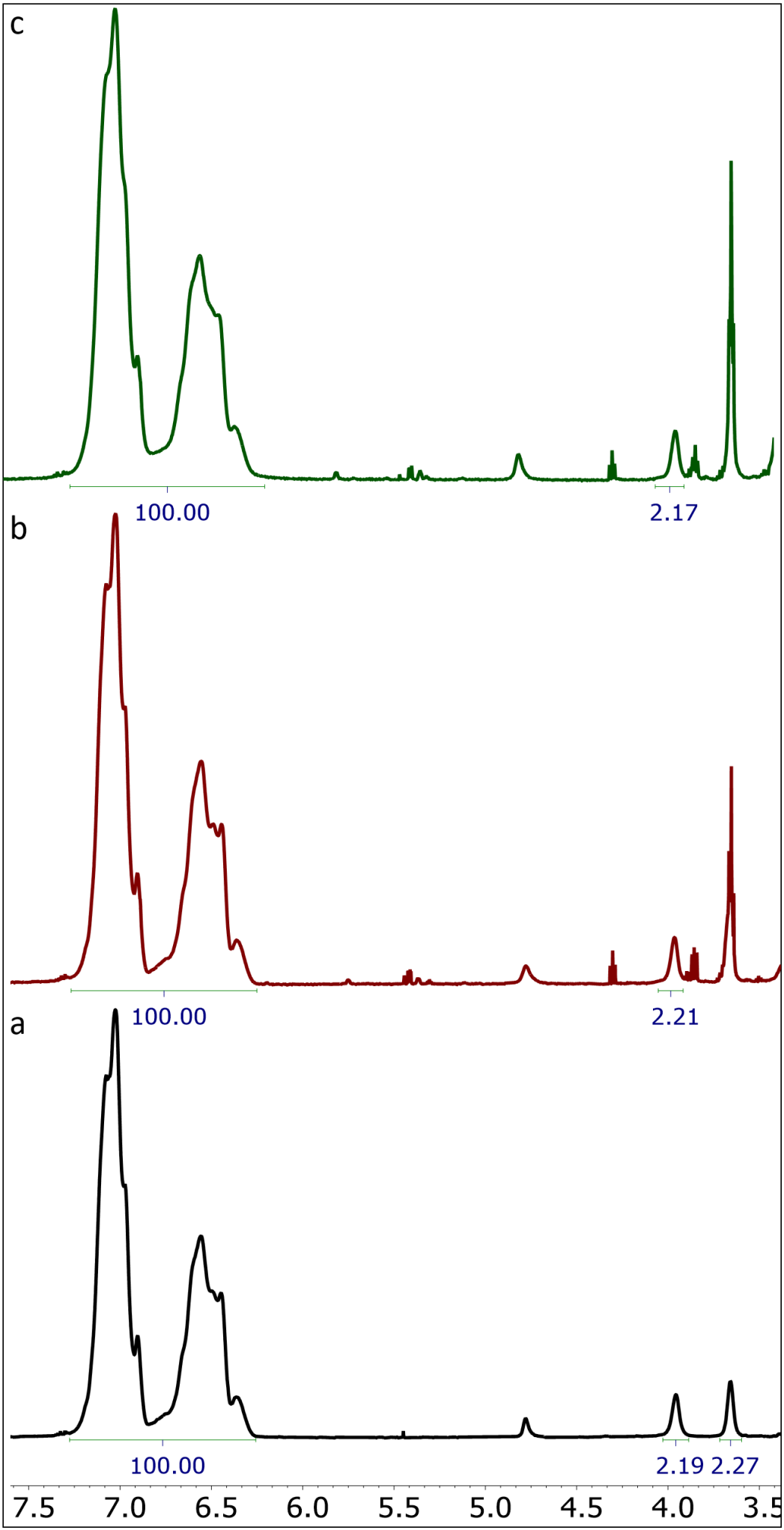
c
100.00
2.17
b
100.00
2.21
a
100.00
2.19 2.27
7.5
7.0
6.5
6.0
5.5
5.0
4.5
4.0
3.5

Fig. S15. ^{1}H-NMR spectra of a) PS_{94}-*b*-$PHEMA_6^{149}$ polymer before pH treatment; b) PS_{94}-*b*-$PHEMA_6^{149}$ polymer treated at pH 13 for 20 min; c) PS_{94}-*b*-$PHEMA_6^{149}$ polymer treated at pH 13 for 24 h in $CDCl_3$ and DMSO-d6 (volume ratio of 1/1) with internal standard TMS.

We have investigated the possibility of hydrolysis of the HEMA moieties of PS_{94}-*b*-$PHEMA_6^{149}$ polymer by immersing it in a pH 13 solution for 20 minutes (duration of water permeance measurement at each pH) and 24 hours respectively. No hydrolysis of PS_{94}-*b*-$PHEMA_6^{149}$ polymer occurred even after 24 hour exposure to pH 13 aqueous solution.

V. Retention measurements

The rejection measurements were accessed in a dead-end mode with continuously stirring under a trans-membrane pressure of 2 bar at 20 °C (**Fig. S14**). The membrane testing cell is purchased from EMD Millipore™ and refitted to our house-made devices. The effective membrane area was 1.77 cm^2. Each measurement was conducted in triplicate.

The retention properties of the membranes were investigated using bovine serum albumin (BSA), hemoglobin (HB) and catalase (CAT). The feed solution of proteins was all freshly prepared in phosphate-buffered saline (PBS, pH = 7.4) for retention measurement. PBS solution was first supplied to the membranes for 1 h at the trans-membrane pressure of 2 bar in order to exclude the influence of buffer, and then the 1 g L^{-1} feed solution of proteins was provided at the same pressure for 2 h.

The concentration of proteins in the feed (C_f) and permeate (C_p) was determined by UV-vis spectrophotometer (GENESYS 10S, Thermo Scientific) and the retention rate was calculated following the equation showed below:

$$R\% = \left(1 - \frac{C_p}{C_f}\right) \times 100\% \tag{11}$$

Where, C_p and C_f are concentrations of proteins in permeate and feed, respectively.

Solute transmission is usually expressed in terms of the observed percentage transmission (τ_{Obs}).[7]

$$\tau_{Obs} = \frac{C_p}{C_f} \times 100 \tag{12}$$

The selectivity (ψ) of one protein from another one is expressed as:[7]

$$\psi = \frac{(\tau_{Obs})_i}{(\tau_{Obs})_j} \tag{13}$$

where $(\tau_{Obs})_i$and $(\tau_{Obs})_j$are the observed percentage transmission of two different proteins.

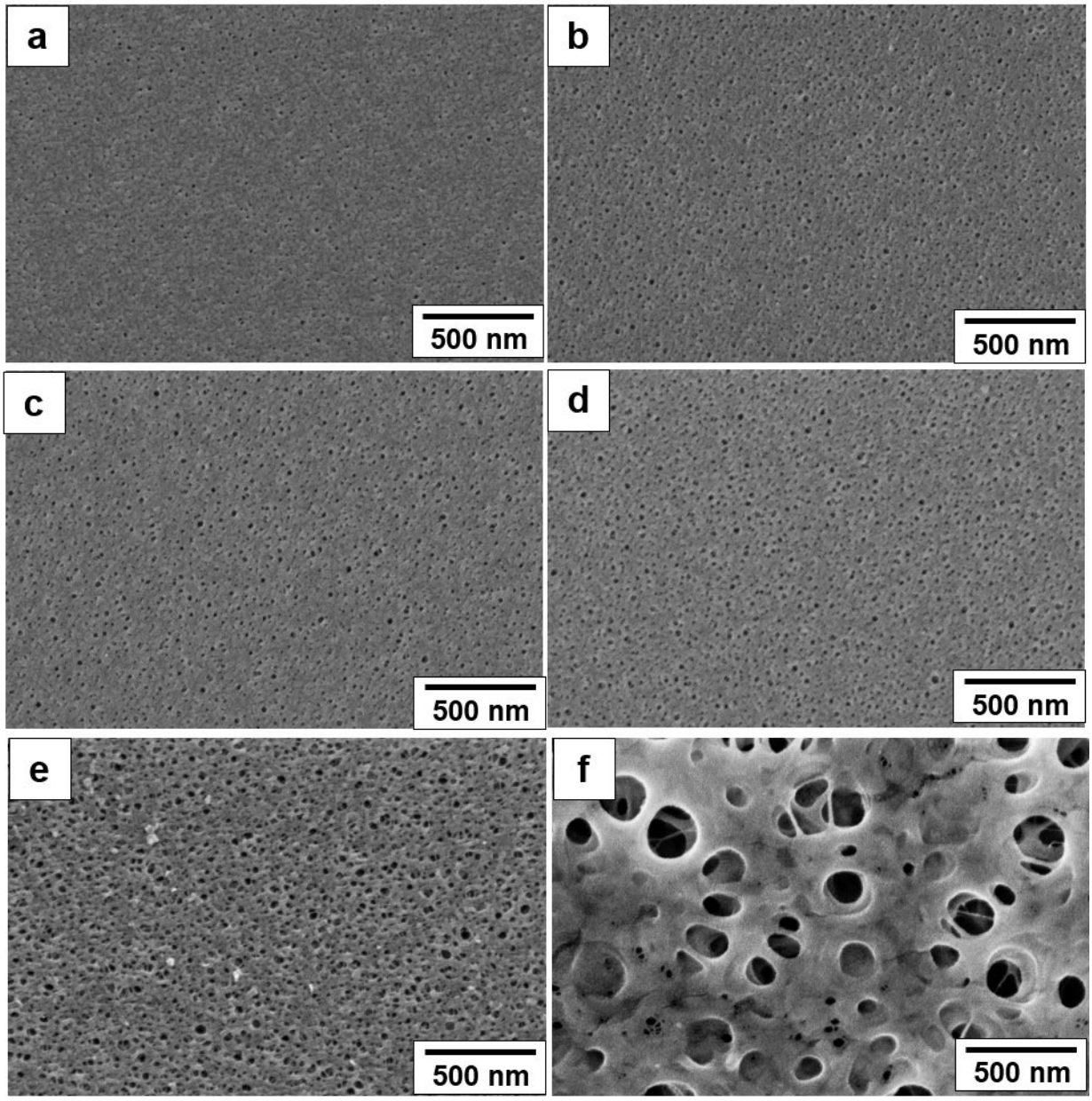

Fig. S16. SEM images of (a) PAN-19/002 (b) PAN-02/141 (c) H-PAN-01/87 (d) PAN-HV2-5 (e) PAN-8 (f) PAN-6 membrane surfaces

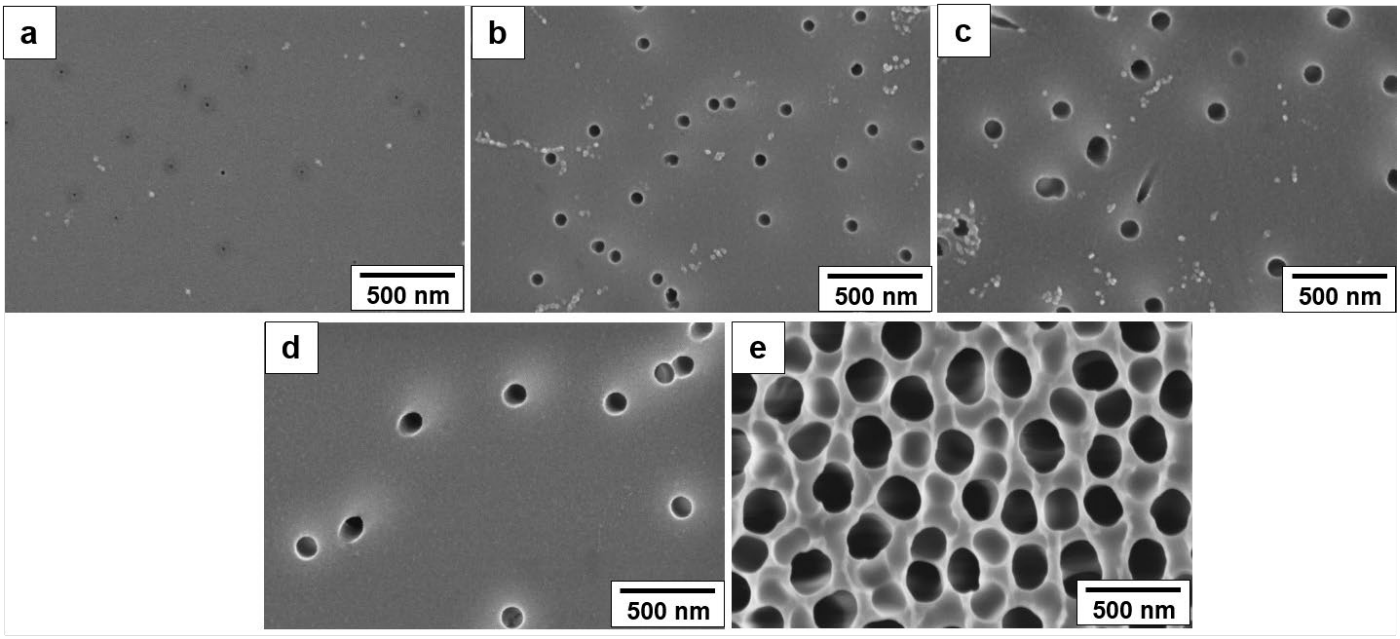

Fig. S17. SEM images of (a) PC_0.015 (b) PC_0.05, (c) PC_0.08, (d) PC_0.1, (e) Anodisc membrane surface

Table S7. Protein retention of membranes in 1 g/L feed solution at pH 7.4.

Membrane	BSA		Hb		Cat	
	Permeance [L h^{-1} m^{-2} bar^{-1}]	Retention [%]	Permeance [L h^{-1} m^{-2} bar^{-1}]	Retention [%]	Permeance [L h^{-1} m^{-2} bar^{-1}]	Retention [%]
PS-*b*-P(HEMA-*r*-SEMA)	183 ± 9	20.48 ± 1.75	32 ± 2	95.09 ± 0.38	8 ± 2	97.02 ± 1.47
Anodisc	48 ± 1	23.36 ± 8.74	19 ± 2	17.87 ± 5.42	9 ± 4	92.20 ± 5.86
PC_0.015	1 ± 0	76.48 ± 1.46	1 ± 0	73.57 ± 8.73	1 ± 0	90.24 ± 0.14
PC_0.05	28 ± 4	60.74 ± 7.59	19 ± 4	42.68 ± 6.17	8 ± 0	98.12 ± 0.44
PC_0.08	28 ± 2	76.95 ± 1.84	15 ± 0	78.98 ± 3.47	9 ± 2	98.83 ± 0.88
PC_0.1	20 ± 2	87.36 ± 2.24	16 ± 1	61.10 ± 6.71	7 ± 1	98.09 ± 0.24
PAN-19/002	32 ± 2	98.77 ± 0.87	14 ± 7	97.51 ± 0.70	8 ± 0	97.44 ± 0.32
PAN-02/141	36 ± 3	99.66 ± 0.33	10 ± 1	98.50 ± 0.11	10 ± 1	99.60 ± 0.41
H-PAN-01/87	44 ± 3	98.27 ± 1.26	15 ± 4	98.01 ± 0.35	11 ± 3	99.95 ± 0.05
PAN-HV2-5	44 ± 4	99.29 ± 0.61	14 ± 3	99.33 ± 0.31	12 ± 2	98.96 ± 1.04
PAN-8	36 ± 2	95.65 ± 4.03	14 ± 2	98.62 ± 0.37	6 ± 2	99.73 ± 0.38
PAN-6	41 ±9	54.63 ± 12.63	19 ± 0	73.74 ± 1.27	9 ± 2	98.89 ± 0.01
PAN_PY	15 ± 5	96.55 ± 4.88	10 ± 5	97.91 ± 0.23	12 ± 2	98.47 ± 1.53

PAN_PX	34 ± 4	99.00 ± 1.00	19 ± 3	98.54 ± 0.83	17 ± 10	98.64 ± 0.92
PSUH	49 ± 12	98.12 ± 0.58	10 ± 1	96.20 ± 0.71	7 ± 2	97.94 ± 0.92
PES_LY	41 ± 5	98.87 ± 0.09	11 ± 2	98.48 ± 1.27	10 ± 0	99.91 ± 0.01
PES_UE	9 ± 1	98.80 ± 0.89	5 ± 1	99.72 ± 0.09	7 ± 1	99.50 ± 0.04
PES_LX	29 ± 4	97.23 ± 0.79	11 ± 0	100 ± 0	8 ± 1	99.44 ± 0.11
PVDF_V5	52 ± 15	92.53 ± 4.39	22 ± 4	98.52 ± 0.17	13 ± 1	97.71 ± 1.61
PVDF_BX	48 ± 4	79.10 ± 17.10	27 ± 5	90.23 ± 7.45	7 ± 2	96.20 ± 2.97
PVDF_A6	50 ± 12	95.14 ± 1.32	21 ± 1	99.57 ± 0.44	8 ± 0	98.52 ± 0.38
PVDF_V6	29 ± 4	99.52 ± 0.58	17 ± 4	99.82 ± 0.18	10 ± 1	99.05 ± 0.17
RC	35 ± 4	99.50 ± 0.36	21 ± 4	92.78 ± 5.46	13 ± 6	97.18 ± 0.19

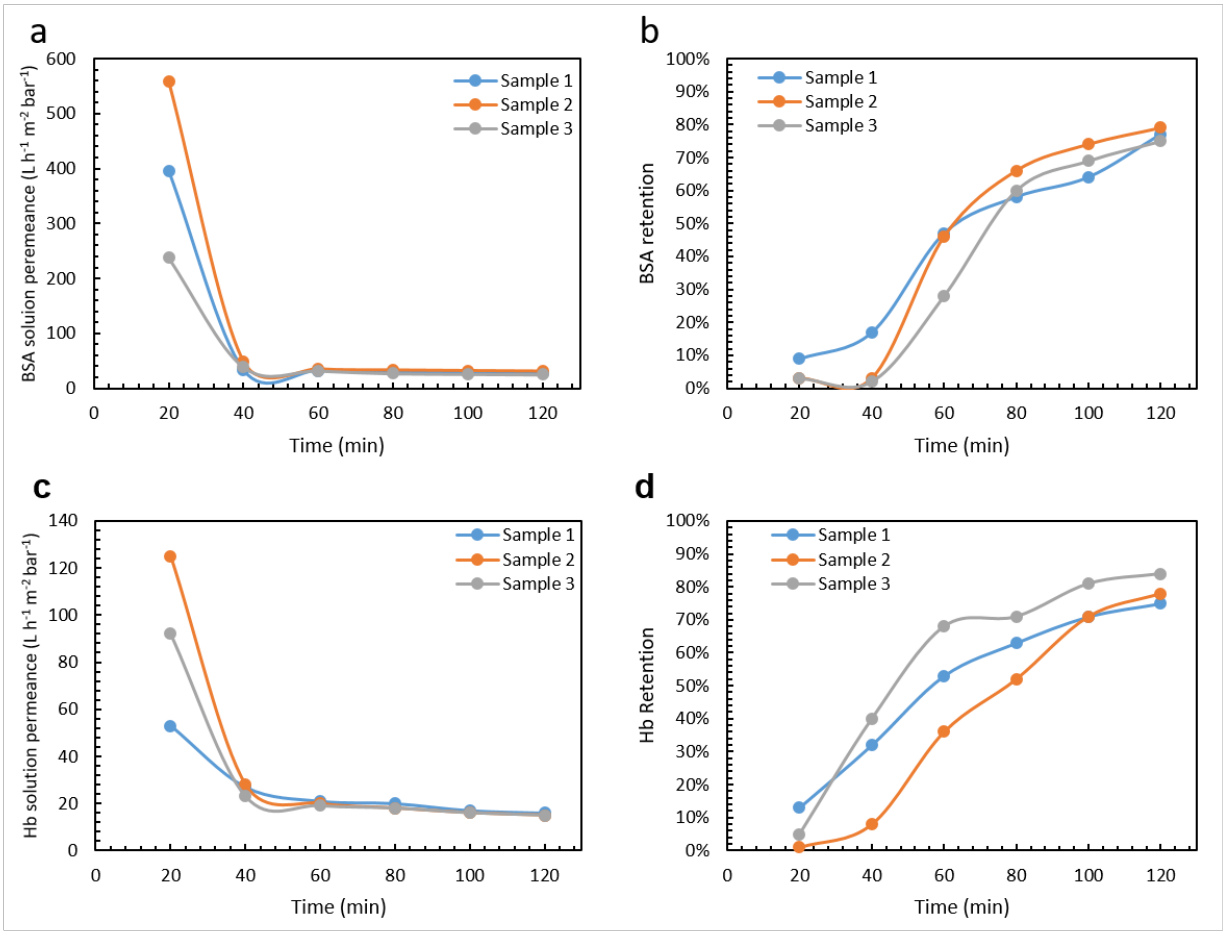

Fig. S18. (a) BSA solution permeance, (b) BSA retention, (c) HB solution permeance and (d) HB retention of PC_0.08 membranes as a function of time for each individual sample.

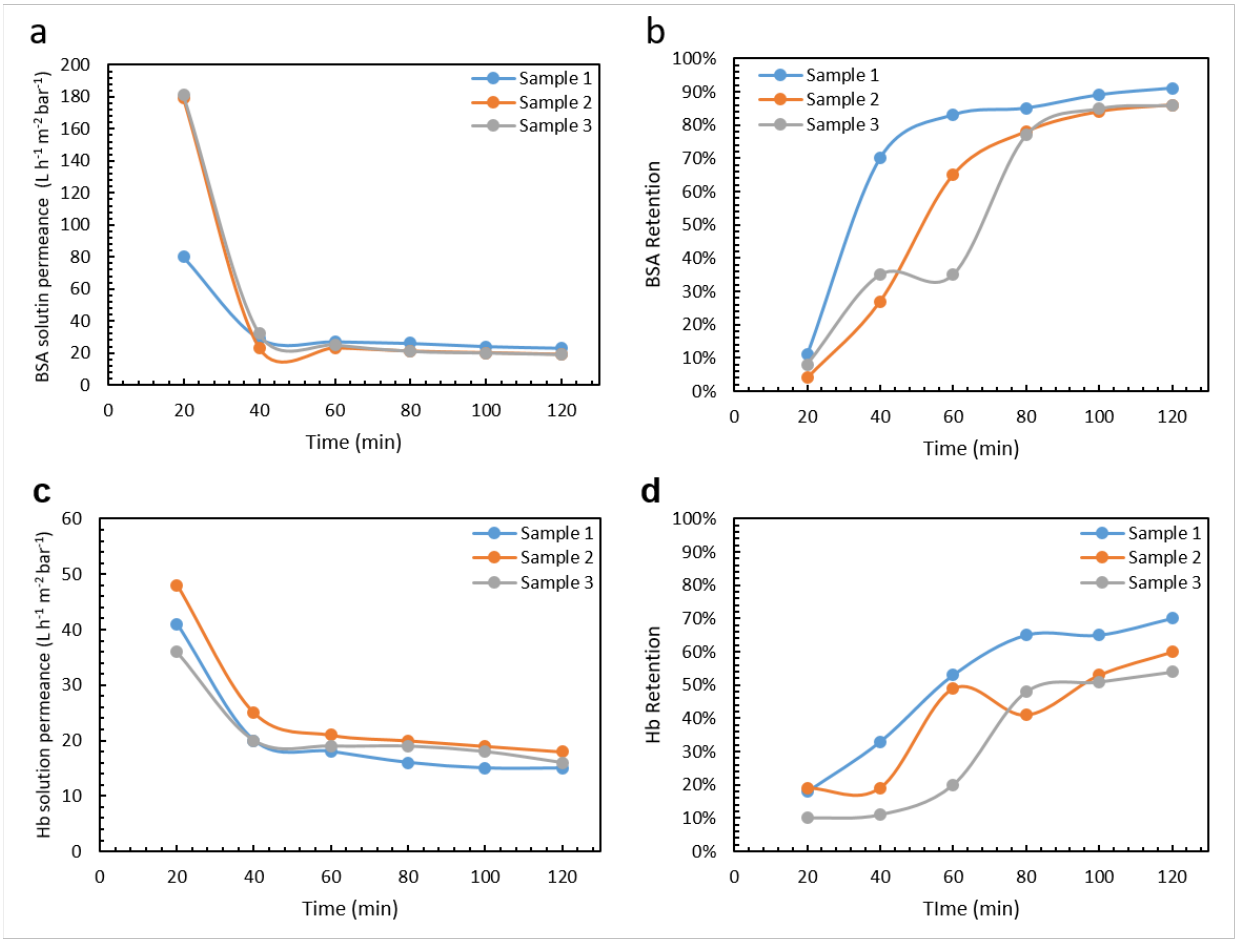

Fig. S19. (a) BSA solution permeance, (b) BSA retention, (c) HB solution permeance and (d) HB retention of PC_0.1 membranes as a function of time for each individual sample

References

[1] A. Hirao, H. Kato, K. Yamaguchi, S. Nakahama, Polymerization of monomers containing functional groups protected by trialkylsilyl groups. 5. Synthesis of poly (2-hydroxyethyl methacrylate) with a narrow molecular weight distribution by means of anionic living polymerization, Macromolecules, 19 (1986) 1294-1299.
[2] J. Wang, M.M. Rahman, C. Abetz, S. Rangou, Z. Zhang, V. Abetz, Novel Post-Treatment Approaches to Tailor the Pore Size of PS-b-PHEMA Isoporous Membranes, Macromolecular rapid communications, 39 (2018) 1800435.
[3] X. Bories-Azeau, S.P. Armes, H.J. van den Haak, Facile synthesis of zwitterionic diblock copolymers without protecting group chemistry, Macromolecules, 37 (2004) 2348-2352.
[4] C.M. Hansen, Hansen solubility parameters: a user's handbook, CRC press, 2007.
[5] D.W. Van Krevelen, K. Te Nijenhuis, Properties of polymers: their correlation with chemical structure; their numerical estimation and prediction from additive group contributions, Elsevier, 2009.
[6] C. Hou, S. Lin, F. Liu, J. Hu, G. Zhang, G. Liu, Y. Tu, H. Zou, H. Luo, Synthesis of poly (2-hydroxyethyl methacrylate) end-capped with asymmetric functional groups via atom transfer radical polymerization, New Journal of Chemistry, 38 (2014) 2538-2547.
[7] R. Ghosh, Z. Cui, Fractionation of BSA and lysozyme using ultrafiltration: effect of pH and membrane pretreatment, Journal of Membrane Science, 139 (1998) 17-28.